Arabidopsis VASCULAR-RELATED UNKNOWN PROTEIN1 Regulates Xylem Development and Growth by a Conserved Mechanism That Modulates Hormone Signaling[1][W][OPEN]

Etienne Grienenberger and Carl J. Douglas*

Department of Botany, University of British Columbia, Vancouver, British Columbia, Canada V6T 1Z4

Despite a strict conservation of the vascular tissues in vascular plants (tracheophytes), our understanding of the genetic basis underlying the differentiation of secondary cell wall-containing cells in the xylem of tracheophytes is still far from complete. Using coexpression analysis and phylogenetic conservation across sequenced tracheophyte genomes, we identified a number of Arabidopsis (*Arabidopsis thaliana*) genes of unknown function whose expression is correlated with secondary cell wall deposition. Among these, the Arabidopsis *VASCULAR-RELATED UNKNOWN PROTEIN1* (*VUP1*) gene encodes a predicted protein of 24 kD with no annotated functional domains but containing domains that are highly conserved in tracheophytes. Here, we show that the *VUP1* expression pattern, determined by promoter-β-glucuronidase reporter gene expression, is associated with vascular tissues, while *vup1* loss-of-function mutants exhibit collapsed morphology of xylem vessel cells. Constitutive overexpression of *VUP1* caused dramatic and pleiotropic developmental defects, including severe dwarfism, dark green leaves, reduced apical dominance, and altered photomorphogenesis, resembling brassinosteroid-deficient mutants. Constitutive overexpression of *VUP* homologs from multiple tracheophyte species induced similar defects. Whole-genome transcriptome analysis revealed that overexpression of *VUP1* represses the expression of many brassinosteroid- and auxin-responsive genes. Additionally, deletion constructs and site-directed mutagenesis were used to identify critical domains and amino acids required for *VUP1* function. Altogether, our data suggest a conserved role for *VUP1* in regulating secondary wall formation during vascular development by tissue- or cell-specific modulation of hormone signaling pathways.

Plant vascular systems are essential for conducting water, nutrients, and signaling molecules throughout the plant and provide mechanical strength to sustain the extensive upright growth needed to compete for sunlight. Vascular development involves the formation of provascular cells that give rise to the procambium, from which the conducting cells of xylem and phloem differentiate (Steeves and Sussex, 1989). During this process, some procambial cells may remain in their undifferentiated states and function as cambium cells to produce secondary vascular tissues, evident in woody plants such as trees (Sachs, 1981; Busse and Evert, 1999a, 1999b). Physiological, genetic, and molecular studies using Arabidopsis (*Arabidopsis thaliana*) or *Zinnia elegans* xylogenic cells have revealed the involvement of hormonal regulators and transcription factors that may govern vascular tissue differentiation. The phytohormone auxin defines the procambial strand location in a self-reinforcing canalization process (Sachs, 1981; Sachs, 1991), but many studies have pinpointed the role of other hormones, including brassinosteroids (BRs) and GA, in xylem differentiation and development (Nagata et al., 2001; Ohashi-Ito et al., 2002, 2005; Ohashi-Ito and Fukuda, 2003; Cano-Delgado et al., 2004; Tokunaga et al., 2006; Yamamoto et al., 2007; Ragni et al., 2011; Dayan et al., 2012). In addition, molecular and genetic studies in Arabidopsis have revealed transcriptional networks controlling vascular differentiation. Among these, the homeodomain leucine-rich repeat class III (*HD-Zip III*) transcription factors play roles in defining xylem cell fate (for review, see Schuetz et al., 2013). They are mainly expressed in procambial and xylem precursor cells and promote early steps of xylem differentiation (Eshed et al., 2001; Ilegems et al., 2010). NAC (for NO APICAL MERISTEM [NAM], ARABIDOPSIS TRANSCRIPTION ACTIVATION FACTOR1/2 [ATAF1/2], and CUP-SHAPED COTYLEDON2 [CUC2]) domain transcription factors such as VASCULAR-RELATED NAC DOMAIN7 (VND7) and VND6 act as positive master regulators of xylem vessel differentiation (Kubo et al., 2005; Yamaguchi et al., 2008), activating developmental programs of secondary cell wall biosynthesis (Zhong et al., 2008, 2010b; Ohashi-Ito et al., 2010; Yamaguchi et al., 2011; Li et al., 2012; Schuetz et al., 2013).

Defects in xylem secondary cell wall structural integrity are often characterized by a collapse of xylem vessels, and this *irregular xylem* (*irx*) phenotype has been described for several Arabidopsis mutants defective in

[1] This work was supported by the Natural Sciences and Engineering Research Council of Canada (Discovery Grant to C.J.D. and CREATE training grant Working on Walls).

* Address correspondence to carl.douglas@ubc.ca.

The author responsible for distribution of materials integral to the findings presented in this article in accordance with the policy described in the Instructions for Authors (www.plantphysiol.org) is: Carl J. Douglas (carl.douglas@ubc.ca).

[W] The online version of this article contains Web-only data.

[OPEN] Articles can be viewed online without a subscription.

www.plantphysiol.org/cgi/doi/10.1104/pp.114.236406

the biosynthesis of cellulose (Turner and Somerville, 1997; Taylor et al., 1999), hemicellulose (Persson et al., 2007; Li et al., 2012), and lignin (Jones et al., 2001; Hoffmann et al., 2004) as well as for mutants of transcriptional regulators controlling secondary cell wall formation (Brown et al., 2005; Li et al., 2012). Genetic screens for mutants with defective secondary cell walls based on the *irx* phenotype have successfully identified several genes involved in secondary cell wall formation (Turner and Somerville, 1997; Jones et al., 2001). Coexpression analysis can also be used to identify candidate genes involved in a given biological process, and vascular development/secondary cell wall formation has proved particularly amenable to this approach due to the specific spatiotemporal regulation of these processes. Analysis of genes coexpressed with the cellulose biosynthesis genes *IRX5/CELLULOSE SYNTHASE4* (*CESA4*), *IRX3/CESA7*, and *IRX1/CESA8*, marker genes for secondary cell wall deposition (Brown et al., 2005; Persson et al., 2005), led to the discovery of new genes required for this process, including *IRX7/FRAGILE FIBER8*, *IRX8*, *IRX9*, *IRX14*, *IRX10*, *IRX10-LIKE* (*IRX10L*), *PARVUS*, *IRX15*, and *IRX15L* (Zhong et al., 2005; Brown et al., 2007, 2009, 2011; Lee et al., 2007; Peña et al., 2007; Persson et al., 2007; Wu et al., 2009; Jensen et al., 2011). However, only a small proportion of the sets of coexpressed genes reported in several studies has been characterized (Brown et al., 2005; Persson et al., 2005; Ubeda-Tomas et al., 2007; Oikawa et al., 2010).

Approximately 65% of the Arabidopsis genes are members of gene families (Arabidopsis Genome Initiative, 2000), suggesting a large potential for functional redundancy. In several cases where functional studies have been performed on genes belonging to gene families, a mutation in any one of the closely related genes has been found to result in no or subtle morphological defects. Double or higher order mutants are needed to uncover the in vivo functions of these genes (Grienenberger et al., 2010; Kim et al., 2010), rendering difficult the functional characterization of novel genes. Another challenge in deciphering the biological functions of genes in model systems such as Arabidopsis is presented by novel gene families that lack similarity to any genes of known function. Annotation of the Arabidopsis genome suggests that 30% to 34% of the genes are predicted to encode either hypothetical proteins or proteins of unknown function (Lamesch et al., 2012). Previous studies have identified many genes of unknown function that are tightly coexpressed with secondary cell wall-related genes (Brown et al., 2005; Persson et al., 2005; Oikawa et al., 2010), suggesting that potentially novel functions are involved in vascular development or secondary cell wall formation.

To date, 41 green plant genomes are available in the Phytozome version 9.1 database (www.phytozome.net) representing key phylogenetic nodes of plant evolution from green algae to flowering plants. Gene conservation within evolutionary clusters is thus easy to evaluate and provides a new dimension to analyzing gene functions. Despite a great variety of patterns in vascular systems and organs, many studies suggest the conservation of mechanisms that underlie the vascular tissue formation tracheophytes (Weng and Chapple, 2010; Zhong et al., 2010a; Hörnblad et al., 2013). Genes involved in fundamental processes of vascular system formation are thus expected to be strictly conserved among vascular plants, and phylogenetic comparisons provide a new tool to predict novel gene functions that may be involved in this process.

Here, we report the identification of four Arabidopsis genes, *At3g21710/VASCULAR-RELATED UNKNOWN PROTEIN1* (*VUP1*) and its homologs *At1g50930/VUP2*, *AT3G20557/VUP3*, and *AT5G54790/VUP4*, encoding novel proteins that show no sequence or structural similarities to any functionally characterized proteins in reference databases. We identified *VUP1* by coexpression and phylogenetic analyses. Loss-of-function *vup1* mutants exhibit *irx* vessel defects, suggesting an involvement in xylem and/or secondary cell wall formation. Functional study of *VUP1* by constitutive overexpression revealed pleiotropic defects of plant development, including a severe dwarfism, dark green leaves, and reduced apical dominance. Whole-genome expression profiling and overexpression of *VUP1* in BR signaling and other mutant backgrounds provided indirect evidence of a role for *VUP1* in BR-dependent signal transduction, possibly downstream of the convergence with GA and PHYTOCHROME B (PHYB) signaling pathways. Structure-function analysis shows that VUP1 molecular function is highly conserved across tracheophytes and is based on a few critical conserved residues, some of which are modified by phosphorylation. Altogether, these results suggest that VUP1 and its close homologs may act as regulatory proteins by mediating BR-dependent signal transduction and that VUP1 is specifically involved in xylem development.

RESULTS

Bioinformatic Approach to Identify Vascular-Related Genes of Unknown Function

In an effort to identify novel genes that may play roles in plant vascular and secondary cell wall development, we used bioinformatic approaches based on coexpression analysis and phylogenetic conservation. We first selected about 200 genes strongly coregulated ($r^2 > 0.7$ in the BioArray Resource for Plant Biology Expression Angler; Toufighi et al., 2005) with three genes known for their roles in secondary cell wall formation: *CESA8*, encoding a secondary cell wall-specific cellulose synthase subunit (Turner and Somerville, 1997); *KNOTTED-LIKE HOMEOBOX OF ARABIDOPSIS THALIANA7*, a transcriptional regulator of secondary cell wall formation (Brown et al., 2005; Li et al., 2012); and *HYDROXYCINNAMOYL-COENZYME A SHIKIMATE/QUINATE HYDROXYCINNAMOYL TRANSFERASE*, encoding an enzyme required for lignin biosynthesis (Hoffmann et al., 2004). Next, this set of coregulated genes was analyzed for conservation among vascular plants (tracheophytes) by comparing their sequences with genomes in the Phytozome version 9.0

database (www.phytozome.net; Goodstein et al., 2012), which contains sequences of 34 tracheophyte species and six nontracheophyte genomes (from green algae and the bryophyte *Physcomitrella patens*). Arabidopsis genes in the coregulated list conserved in all Phytozome genomes with an arbitrary BLAST (Altschul et al., 1997) E-value cutoff of 1e-50 were selected. Proteins with lower similarity were analyzed individually, and genes encoding proteins without obvious orthologs in other tracheophytes were removed. Among them was the *VUP1*/*At3g21710* gene, and we report here its functional characterization.

VUP1 Is Conserved and Restricted to Vascular Plants

Two splice variants are predicted for *VUP1*/*At3g21710* by The Arabidopsis Information Resource 10 database, *VUP1.1*, with two exons and one intron, and *VUP1.2*, with three exons and two introns (Fig. 1A). The corresponding encoded proteins share 150 amino acids at the N terminus but have different C termini. In order to evaluate the expression level of each variant in different regions of inflorescence stems and from mature leaves, we employed reverse transcription (RT)-PCR and splice variant-specific primers. As shown in Figure 1B, the *VUP1.2*-specific amplicon was abundant while the *VUP1.1*-specific amplicon was detected at low levels. This shows that *VUP1.2* is the major *VUP1* splice variant in the organs assayed, consistent with its high abundance in EST databases and in complementary DNA (cDNA) collections. We use the *VUP1.2* transcript synonymously with *VUP1* in the subsequent presentation unless otherwise specified.

VUP1 is predicted to encode a novel protein of 211 amino acids and 23.7 kD. Neither a signal peptide nor a transmembrane domain was found using SignalP and TMHMM software (Krogh et al., 2001; Bendtsen et al., 2004), and database searches did not reveal similarity with any characterized proteins outside of VUP1 homologs or the presence of any annotated functional domains. Three *VUP1* homologs were found encoded by the Arabidopsis genome, which we designed *VUP2* (*At1g50930*), *VUP3* (*At3g20557*), and *VUP4* (*At5g54790*).

Extensive searches in genomic and EST databases showed that proteins with sequence similarity to Arabidopsis VUP1 are present in every genome of vascular plants for which genome or EST sequences are available, including all 33 other tracheophyte genome sequences in Phytozome version 9.0 mentioned previously (Fig. 2A), suggesting a strict conservation of *VUP1* in this evolutionary lineage. Interestingly, no homologs were found encoded by genomes of *P. patens* or the six green algae curated at the Phytozome 9.0 database, nor did we find them in animals, fungi, or bacteria by querying the National Center for Biotechnology Information nonredundant database. Thus, *VUP1* appears to be specific to vascular plant species. We found that *VUP1* homologs are often part of small gene families of no more than four members. In some species, they appear to be unique genes (Fig. 2A), but we did not exhaustively search genomes of these species for potential nonannotated VUP1 homologs.

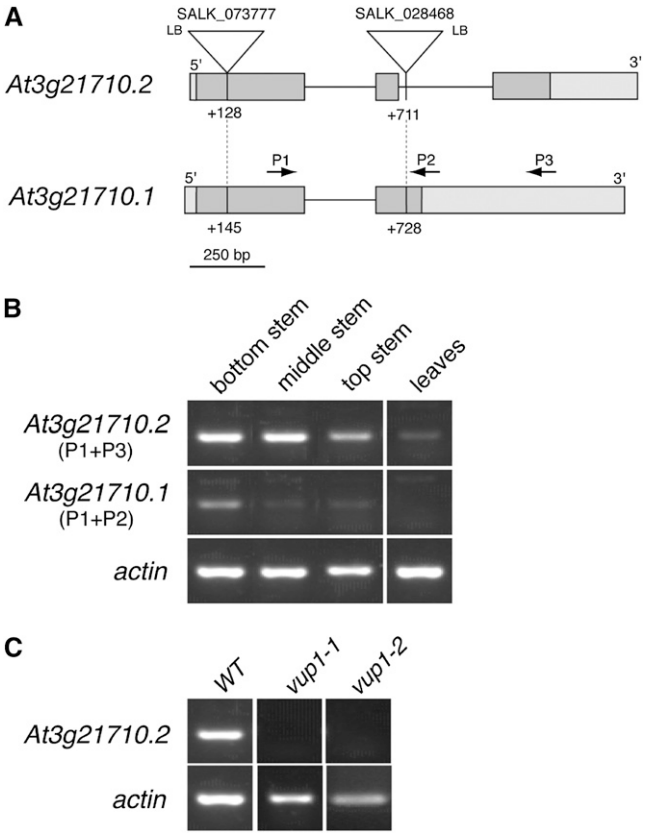

Figure 1. Molecular characterization of *At3g21710*/*VUP1* splice variant and insertion alleles. A, Diagram of the Arabidopsis *VUP1* gene and its predicted splice variants (*At3g21710.1*/*VUP1.1* and *At3g21710.2*/*VUP1*), showing the positions of exons (dark gray boxes), introns (lines), 5′- and 3′-untranslated regions (light gray boxes), and the T-DNA insertion sites (triangles). Primer annealing sites used for splice variant-specific PCR are indicated by arrows. LB, Left border. B, Expression of *VUP1* splice variants in stems and rosette leaves of 8-week-old plants (bottom, 0–3 cm; middle, 6–9 cm; and top, 10–15 cm from the bottom of inflorescence stems). *ACTIN2* expression was monitored as a control. C, RT-PCR detection of *At3g21710.2*/*VUP1* transcripts in wild-type (WT; Col-0), *vup1-1* (SALK_073777C), and *vup1-2* (SALK_028468) stems. *ACTIN2* expression was monitored as a control.

To investigate the sequence conservation between VUP1 homologs, protein sequences from multiple species were aligned using MUSCLE 3.7 (Edgar, 2004b). The multialignment showed an overall low conservation between homologous sequences (35%–50% similarity), with highly divergent regions, but revealed the presence of four highly conserved motifs of nine to 20 residues containing strictly conserved residues among all homologs (Fig. 2B, asterisks; Supplemental Fig. S1), which we designate as M1 to M4 (Fig. 2B). The *Selaginella moellendorffii* homolog showed the highest divergence in the conserved motifs and in particular lacks several conserved residues in the M3 motif that are present in other homologs (Fig. 2B). While M1 to M3 motifs are strictly conserved in VUP1 homologs, the M4 motif was found

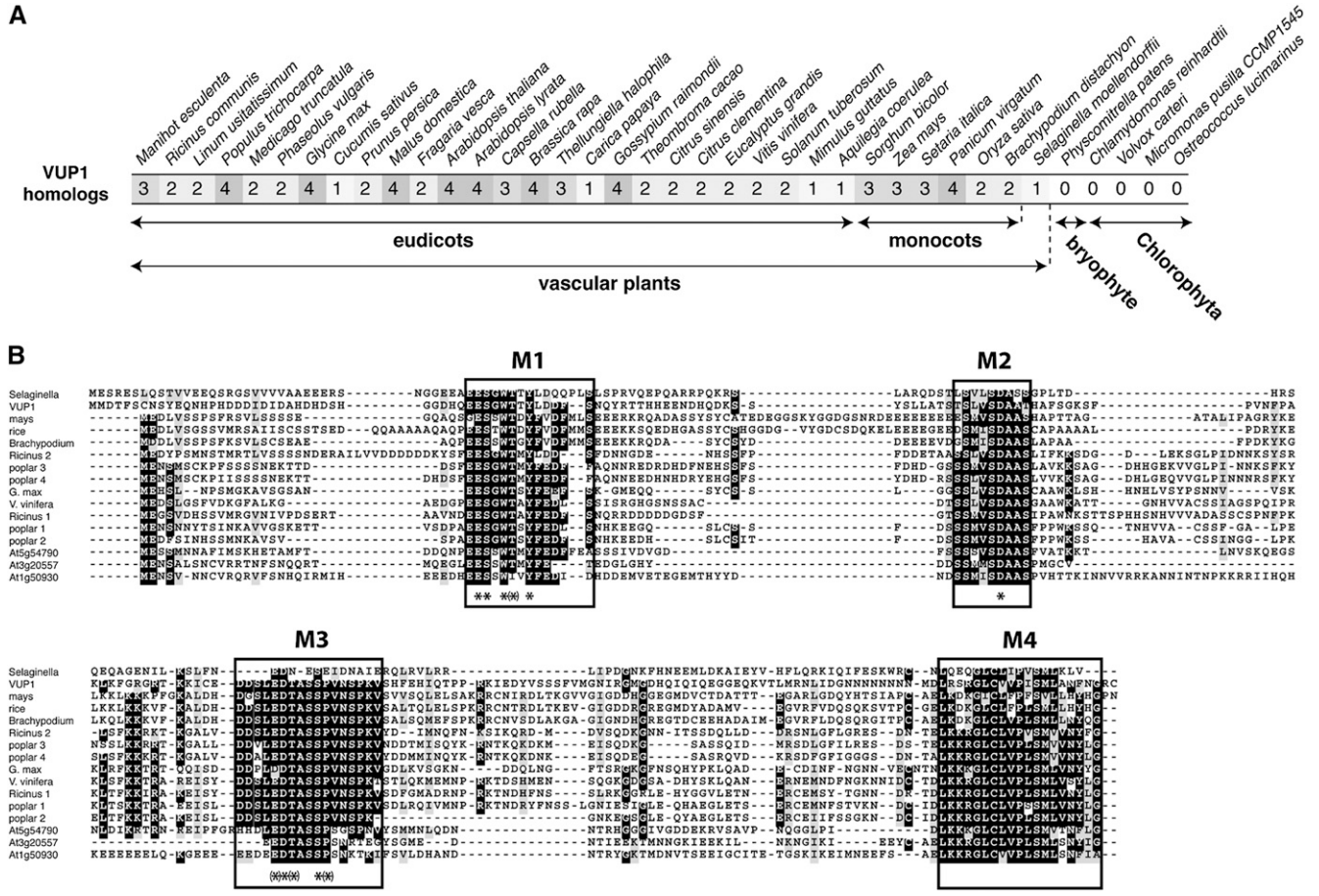

Figure 2. Putative *VUP1* homologs from land plant and green algae species showing multiple sequence alignments. A, Number of putative VUP1 homologs in genomes of various plant and green algae species present in the Phytozome version 9.0 database (www.phytozome.net). Putative homologs were selected based on the overall similarity and the presence of conserved residues. B, Alignment of full-length deduced amino acid sequences of selected VUP1 homologs. Alignments were obtained using the MUSCLE 3.7 program. Conserved and partially conserved residues are marked with black and gray boxes, respectively. M1 to M4 indicate motifs conserved between all homologs. Asterisks indicate strictly conserved residues within all known VUP1 homologs. Asterisks in brackets represent highly conserved residues that are absent in rare cases in some homologs.

to be absent in some homologs (Supplemental Fig. S1). None of those conserved motifs were found encoded by genes other than *VUP1* homologs, with the exception of the M4 motif, which was found partly conserved at the C terminus of several basic helix-loop-helix (bHLH) transcription factors in Arabidopsis and other species (Supplemental Fig. S2). Altogether, these data indicate that *VUP1* encodes a novel protein of unknown function, conserved within and specific to the tracheophyte lineage.

Loss of Function of *VUP1* Results in an *irx* Phenotype

To test a potential role for *VUP1* in vascular development, two transfer DNA (T-DNA) insertion lines (SALK_073777 and SALK_028468, named *vup1-1* and *vup1-2*), with insertions in the first exon and the second intron, respectively, were obtained from the Arabidopsis Biological Resource Center (Alonso et al., 2003), and homozygous lines were generated. RT-PCR was performed to assess *VUP1* expression using cDNA from wild-type and mutant inflorescence stems as templates. Using primers spanning insertion sites (see "Materials and Methods"), RT-PCR showed no detectable *VUP1* transcripts in *vup1-1* and *vup1-2* (Fig. 1C), suggesting that both mutants are loss of function.

Phenotypic analysis of *vup1* mutants did not reveal obvious developmental defects when grown in standard conditions. To view the anatomy and morphology of developing inflorescence stems in *vup1-1* and *vup1-2* mutants relative to the wild type, cross sections from the bases of inflorescence stems of 6-week-old plants were examined. No defects in vascular tissue organization or differences in cell wall thickness were observed; however, xylem vessel cells in both mutants exhibited a consistent collapsed perimeter, or *irx* morphology (Fig. 3, B, D, and E, arrows), relative to the normally round shapes of such

vessels in wild-type plants (Fig. 3, A and C). Around half of *vup1-1* and *vup1-2* *irx* vascular bundles had *irx* vessels (Fig. 3F), suggesting the involvement of *VUP1* in the secondary cell wall deposition and/or xylem development.

VUP1 Expression Pattern and VUP1 Subcellular Localization

To obtain clues about *VUP1* function, we first examined its expression pattern. A translational fusion of the *VUP1* genic sequence to the *GUS* reporter gene under the control of a 2-kb promoter sequence upstream of *VUP1* (*promVUP1*:*VUP1*:*GUS*) was generated and transformed into Arabidopsis. Histochemical staining for GUS activity of T1 plants from seven independent lines showed a consistent expression pattern detected throughout various plant organs in different tissues. GUS activity was mainly found restricted to vascular tissues in cotyledons (Fig. 4A), rosette leaves (Fig. 4, A and K), and the vascular tissues of floral organs (sepals, petals, and anther filaments; Fig. 4I). In young leaves, GUS activity was often weak or not detected, but in many cases it was also observed in leaf meristematic regions (Fig. 4, A and L, arrows). Strong GUS activity was detected in roots but was not restricted to the vascular tissues (Fig. 4B) and was absent from the root tip and the root elongation zone (Fig. 4B). GUS activity was also observed in inflorescence stems, and analysis of cross sections taken at the basal portions of stems (first internode) revealed that GUS activity was restricted to the endodermis layer, between the cortex on one side and the interfascicular fibers or vascular bundles on the other side, and to cells adjacent to or within the metaxylem of vascular bundles (Fig. 4, C, D, F, and G). Similar patterns were observed in cross sections taken from intermediate stem heights (fourth and eighth internodes; Fig. 4, E and H), with little activity observed at the top of the stem (Fig. 4H). Finally, GUS stain was also detected in developing seeds, possibly in the seed coats (Fig. 4J).

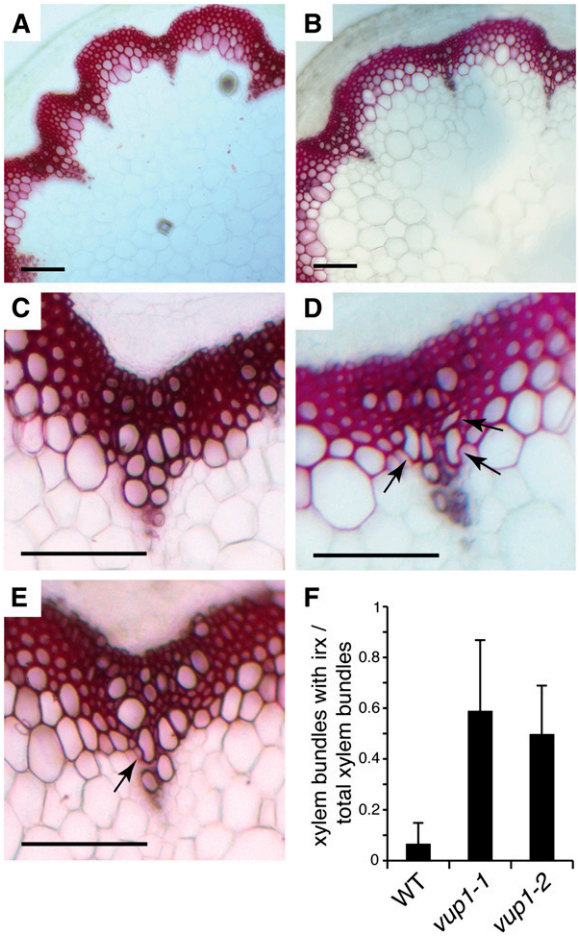

Figure 3. Inflorescence stem phenotype of the Arabidopsis wild type and *vup1* mutants. Cross sections of the basal internodes of 6-week-old stems were stained with phloroglucinol to reveal lignified cell types. A and C, The wild type. B and D, *vup1-1*. E, *vup1-2*. Arrows show *irx* vessel cells. Bars = 100 μm. F, Quantification of the *irx* phenotype in vascular bundles of the basal internode of 6-week-old stems of the wild type (WT), *vup1-1*, and *vup1-2*. n = 20 for the wild type and *vup1-2*; n = 15 for *vup1-1*.

In order to understand where VUP1 may function in the cell, we investigated VUP1 subcellular localization. We generated N- and C-terminal VUP1-YELLOW FLUORESCENT PROTEIN (YFP) translational fusions under the control of the 35S promoter and used the constructs for transient expression in *Nicotiana benthamiana* leaves. As illustrated in Figure 5, A and B, confocal laser microscopy observations revealed YFP fluorescence in different cellular compartments, with a large fraction detected in the nucleus that colocalized with the nuclear marker mCherry-VirD2NLS (Fig. 5, F–H) and was excluded from the nucleolus (Fig. 5, F and H, arrowheads). Weaker fluorescence was also consistently observed in the cytosol, visible in the cell periphery and in cytoplasmic streams (Fig. 5, A and B). Similar results were obtained for the N-terminal fusions (data not shown), and examination of VUP1-YFP localization in the leaves of stably transformed Arabidopsis plants revealed similar localization patterns (Fig. 5, C–E).

To address possible artifactual VUP1-YFP signal localization due to proteolysis of the fusion protein, we assayed its stability in Arabidopsis overexpression lines. Supplemental Figure S3 shows immunoblot analysis of protein extracts taken from leaves of Arabidopsis plants overexpressing *VUP1-YFP*, which revealed partial degradation of the fusion protein. Similar data were obtained from *N. benthamiana* leaves expressing *VUP1-YFP* (data not shown), suggesting that a proportion of the YFP signal seen in *N. benthamiana* could come from partially degraded VUP1-YFP or free YFP, which may not reflect the true VUP1 subcellular localization.

Constitutive Expression of *VUP1* in Arabidopsis Induces Multiple Developmental Defects and Mimics the BR-Deficient Phenotype

To further investigate *VUP1* function, we analyzed the consequences of its ectopic overexpression in

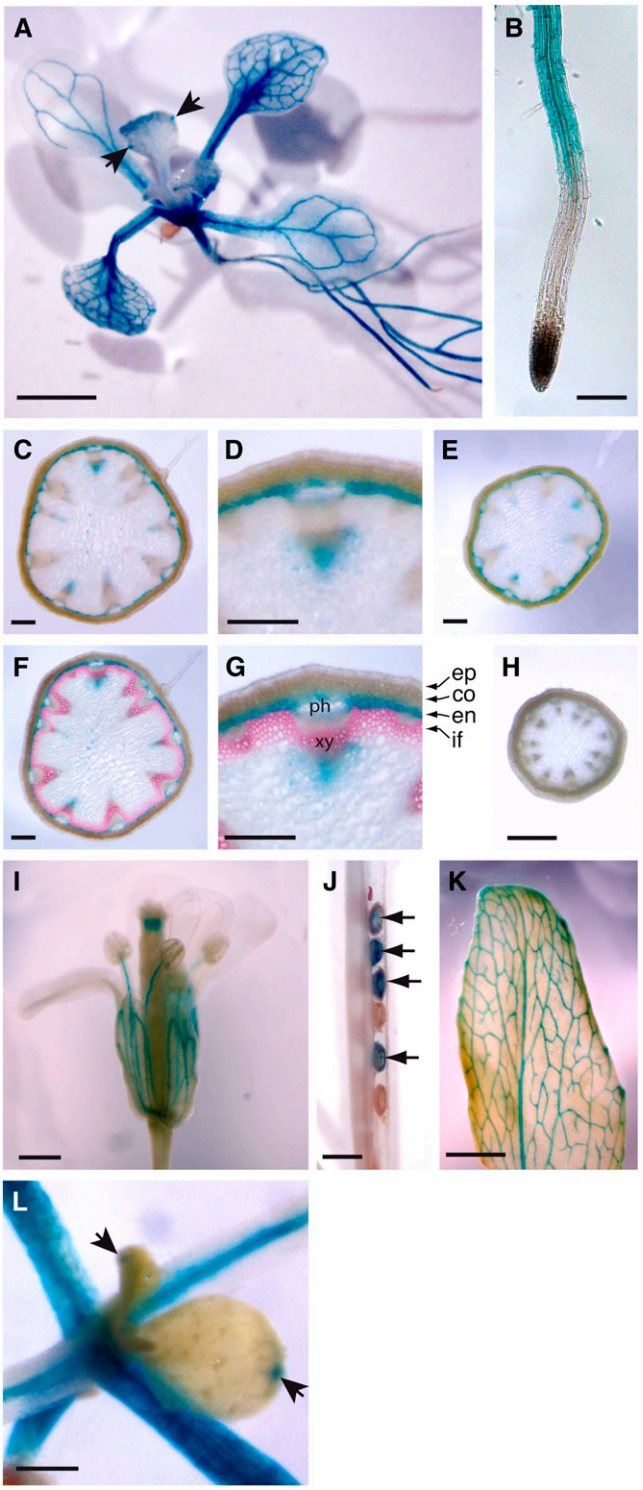

Figure 4. *VUP1* promoter activity. Histochemical localization of GUS activity is shown in *promVUP1*:*VUP1*:*GUS* transgenic plants. The results shown are representative of more than five independent lines. GUS activity is shown in a 10-d-old seedling (A), 7-d-old root (B), cross sections of an 8-week-old inflorescence stem at the first internode (C, D, F, and G), fourth internode (E), and eighth internode (H), fully opened flower (I), developing silique (J), developing rosette leaf (K), and young leaf of a 10-d-old seedling (L). Arrows in L and A show GUS activity in meristematic zones of young leaves; arrows in J indicate developing seeds with GUS activity. co, Cortex; en, endodermis; ep, epidermis; if, interfascicular fibers; ph, phloem; xy, xylem. Bars = 250 μm (A), 150 μm (C–H), 500 μm (I and K), and 100 μm (B, J, and L).

Arabidopsis. A *prom35S*:*VUP1*:*YFP* construct was generated and transformed into Arabidopsis. When analyzing the T1 generation, *VUP1*:*YFP* expression was silenced in a high percentage (about 95%) of lines, as no YFP fluorescence was detected by fluorescence microscopy. However, we isolated more than 15 independent T1 plants in which *VUP1*:*YFP* expression was high (*VUP1* overexpressors; *VUP1 OX*), and all of these plants exhibited consistent pleiotropic phenotypes encompassing a wide range of dramatic defects in both vegetative and reproductive organs. At the seedling stage, *VUP1 OX* plants exhibited a dwarf phenotype with smaller, round-shaped, and darker green cotyledons and leaves and reduced shoot elongation in comparison with wild-type plants (Fig. 6A). Roots were much shorter, slightly twisty and thicker, and were severely compromised in lateral root formation (Fig. 6A). Hypocotyl length was drastically reduced in both light and dark growth conditions (Fig. 6, A and B).

At the rosette stage, *VUP1 OX* plants exhibited a severe dwarf phenotype (Fig. 6, C and D) and, consequently, a drastically reduced rosette size in comparison with the wild type. Leaves were frequently curved or twisted around the time of bolting (Fig. 6F). Development of the inflorescence stem and the transition to flowering were strongly delayed, with *VUP1 OX* lines requiring over 50 d to initiate bolting when grown in a 16-h/8-h photoperiod, compared with 24 d for the wild type (Fig. 6, E–I and L). *VUP1 OX* inflorescence stems were remarkably shorter than the wild type, with reduced apical dominance (Fig. 6, G and H), and floral organs were shorter than in the wild type, although organ identity and numbers were unaffected (Fig. 6I). *VUP1 OX* plants produced viable seeds; however, the fertility was greatly reduced, with only a few seeds per silique. *VUP1 OX* plants grew very slowly, with some dying before reaching maturity in the soil. The surviving plants, however, exhibited extreme longevity of more than 10 months before senescence, in comparison with about 2 months for wild-type plants grown in the same conditions.

Beside the obvious dwarf phenotype, *VUP1 OX* plants also exhibited a dark green color. Quantification of total chlorophyll contents of *VUP1 OX* and wild-type 10-d-old seedlings revealed an approximately 4-fold higher accumulation of chlorophyll in *VUP1 OX* seedlings in comparison with wild-type seedlings (Fig. 6M).

We also examined the dark-grown features of *VUP1 OX* seedlings. Dark-grown wild-type seedlings had a drastically elongated hypocotyl, an apical hook, and unexpanded cotyledons (Fig. 6B). In contrast, *VUP1 OX* seedlings exhibited a short hypocotyl, no apical hook, and open and partially expanded cotyledons (Fig. 6B), revealing a partial deetiolation phenotype in the dark.

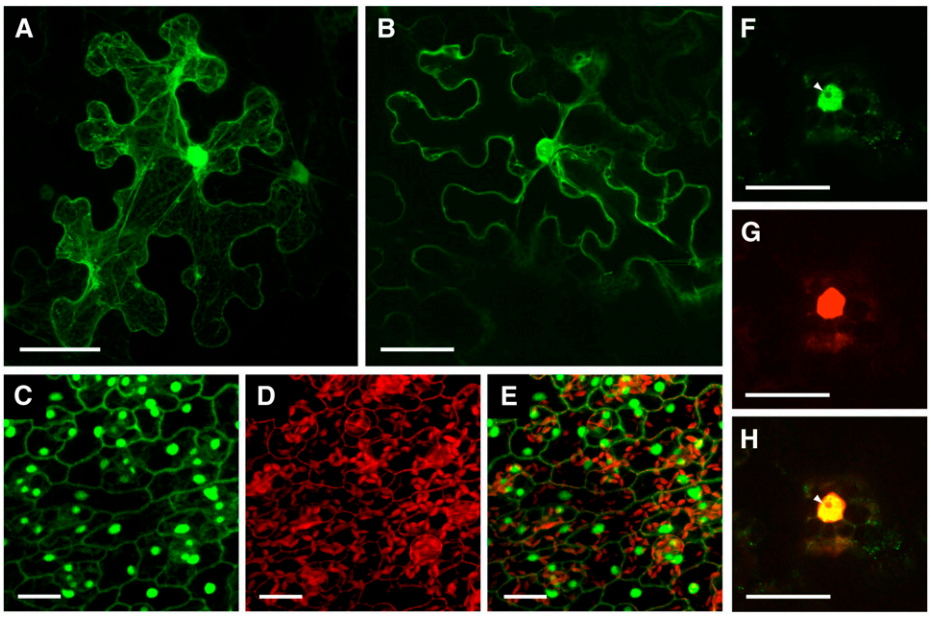

Figure 5. Subcellular localization of VUP1:YFP fusion proteins. A and B, Confocal scanning microscopy observations of *VUP1:YFP* transiently expressed in *N. benthamiana* leaf epidermal cells. Maximum projection image (A) and single optical section (B) of a leaf epidermal cell expressing *VUP1:YFP* are shown. C to E, Confocal scanning microscopy observations of an Arabidopsis leaf expressing a *VUP1:YFP* construct. YFP signal (C), chlorophyll autofluorescence and cell walls stained with propidium iodide (D), and merge of C and D images (E) are shown. F to H, Coexpression of *VUP1:YFP* and *mCherry:VIR2DNLS* (nucleus marker) in *N. benthamiana* leaf epidermal cells. YFP signal (F), mCherry signal (G), and merge of F and G images (H) are shown. Arrowheads indicate the nucleolus. Bars = 40 μm.

Hypocotyl length in etiolated *VUP1 OX* seedlings from two independent lines was nearly one-third that of wild-type plants (Fig. 6N).

The reduced organ size in the *VUP1 OX* plants could be the result of a reduced cell number or cell size. To test these possibilities, we measured the lengths of *VUP1 OX* and wild-type hypocotyl epidermal cells in etiolated seedlings, which revealed an approximately 75% reduction of epidermal cell length in the hypocotyls of *VUP1 OX* plants (Fig. 6O; Supplemental Fig. S4). This correlates with the overall length reduction of hypocotyls (approximately 67%; Fig. 6N) and suggests that the altered hypocotyl growth and organ expansion in *VUP1 OX* plants are largely caused by defective cell elongation.

We also examined the anatomy and tissue organization of *VUP1 OX* inflorescence stems. Transverse sections of 14- and 18-week-old *VUP1 OX* stems stained with phloroglucinol to stain lignified secondary cell walls (Fig. 6K) were compared with those of 8-week-old wild-type stems (Fig. 6J). *VUP1 OX* stems had altered vascular and interfascicular fiber cell shape and patterning, with large lignified phloem fibers at the outer periphery of the phloem, while vascular bundles appeared reduced in size with fewer xylem vessels.

VUP1 OX Seedlings Exhibit Altered Expression of Hormone-Responsive Genes

Many morphological abnormalities observed in the *VUP1 OX* plants, notably dwarfism, hyperaccumulation of chlorophyll, delayed flowering, and constitutive deetiolation, are similar to those observed in mutants with BR deficiencies such as *de-etiolated2* (*det2*) or *brassinosteroid insensitive1* (*bri1*) (Clouse et al., 1996; Kauschmann et al., 1996; Fujioka et al., 1997) or, to a lesser extent, GA-deficient mutants such as *ga1* (Sun et al., 1992). To gain further insight into the function of *VUP1* in plant growth and development and on potential hormone regulatory pathways affected by its misexpression, we carried out a genome-wide transcriptome analysis of *VUP1 OX* 9-d-old seedlings relative to the corresponding wild-type control using a full genome microarray (see "Materials and Methods"). After controlling for consistency between the three normalized biological replicates, a total of 30 and 154 genes were found to be significantly up- and down-regulated, respectively, by at least 1.5-fold in *VUP1 OX* seedlings ($P < 0.01$; Table I; Supplemental Table S1). As expected, *VUP1* was strongly up-regulated (16.6-fold increase over the wild-type level; Table I), but in general, changes were surprisingly moderate given the pronounced *VUP1 OX* phenotype, with only four and 28 genes up- and down-regulated, respectively, by more than 2-fold.

The up-regulated genes were distributed among various functional classes or were functionally uncharacterized (Supplemental Table S1) and did not reveal an obvious trend indicative of perturbation of any particular regulatory or biosynthetic pathway. The 154 down-regulated genes also fell into many functional classes (Supplemental Table S1), but consistent changes in gene expression were observed for functionally related genes, including cell wall-related genes, cell elongation-related genes, and hormone-related genes. Among these, 24 were related to primary cell wall remodeling and/or associated with cell elongation and expansion (Table I). Examples include expansins, xyloglucan endotransglucosylates (XTHs), arabinogalactan proteins (AGPs), Pro-rich proteins, and extensins (Table I). Other genes related to cell elongation were also down-regulated, such as *LONGIFOLIA2* (*LNG2*) and *LNG1*, two homologous genes that promote polar cell elongation by an unknown mechanism (Lee et al., 2006b), and

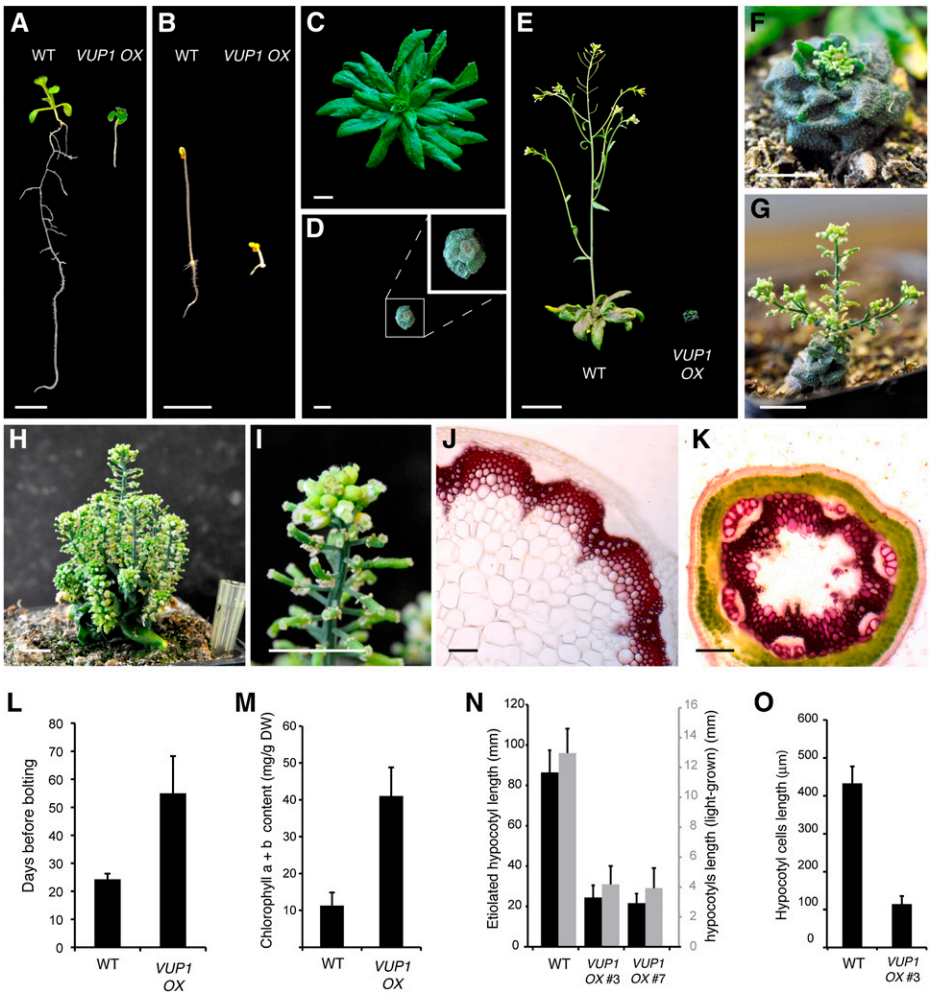

Figure 6. Phenotypes of *VUP1 OX* plants. Results are representative of at least 10 independent lines expressing *prom35S:VUP1:YFP* (*VUP1 OX*). A, Ten-day-old wild-type (WT) and *VUP1 OX* light-grown seedlings. B, Five-day-old wild-type and *VUP1 OX* dark-grown seedlings. C, Four-week-old wild-type plant. D, Four-week-old *VUP1 OX* plant. E, Seven-week-old wild-type and *VUP1 OX* plants. F to I, Seven-week-old (F), 10-week-old (G), and 14-week-old (H and I) *VUP1 OX* plants. J and K, Cross sections of 6-week-old wild-type (J) and 10-week-old *VUP1 OX* (K) inflorescence stems. L, Wild-type and *VUP1 OX* days to bolting in a 16-h/8-h photoperiod ($n = 24$). M, Total chlorophyll contents of wild-type and *VUP1 OX* 10-d-old seedlings. DW, Dry weight. N, Light-grown (gray bars) and etiolated (black bars) hypocotyl lengths of the wild type and two independent *VUP1 OX* T2 lines ($n > 15$). O, Etiolated hypocotyl epidermal cell lengths of the wild type ($n = 25$) and two independent *VUP1 OX* T2 lines ($n = 20$). Error bars represent SD. Bars = 500 μm (A and B), 1 cm (C, D, and F–I), 5 cm (E), and 100 μm (J and K).

the *PHYTOCHROME INTERACTING FACTOR4* (*PIF4*) transcription factor.

In agreement with their roles in cell elongation, many genes annotated as GA, BR, and/or auxin regulated were significantly down-regulated in the *VUP1 OX* seedlings. The GA-responsive gene *GIBBERELLIN-STIMULATED ARABIDOPSIS6* (*GASA6*) and its homolog *GASA4* were strongly down-regulated (fold change = −5.6 and −1.9, respectively; Table I). The expression of both genes is activated by both GA and BR treatment (Sun et al., 2010; Lin et al., 2011). Similarly, expression of the BR-regulated gene *BRASSINOSTEROID ENHANCED EXPRESSION2* (*BEE2*) was down-regulated, as were 16 genes annotated as auxin-responsive genes, including 12 *SMALL AUXIN UP RNA* (*SAUR*) genes and four *INDOLE ACETIC ACID-INDUCED* (*IAA*) genes (Table I).

As cell elongation-related genes are known to be regulated by hormones such as BR, auxin, and GA, we compared the set of *VUP1 OX* down-regulated genes with those previously identified in transcriptome profiling experiments as "BR regulated" (Sun et al., 2010), "auxin (IAA) regulated" (Goda et al., 2004, 2008), and "GA regulated" (Cao et al., 2006). Such comparisons revealed that 44% of the *VUP1 OX* down-regulated genes (68 of 154) were BR-induced genes, while 56% (87 of 154) were BR-regulated genes (induced or repressed; Sun et al., 2010; Fig. 7). Similarly, of the 154 down-regulated genes, 27 were reported as auxin-regulated genes (22 up- and five down-regulated; Goda et al., 2004, 2008) and 21 as GA-regulated genes (17 up- and four down-regulated; Cao et al., 2006). Interestingly, most of the auxin- and GA-regulated genes are also regulated by BR. This is not surprising, as it is known that BR, auxin, and GA have synergistic interactions in elongating tissues and cells (Cohen and Meudt, 1983; Katsumi, 1985; Sala and Sala, 1985) and control an overlapping set of genes (Goda et al., 2004; Nemhauser et al., 2004). Also of note was the observation that most but not all of the *VUP1 OX* down-regulated genes are up-regulated by BR, IAA, and/or GA.

In summary, transcriptome analysis revealed that *VUP1* overexpression down-regulates the expression of a suite of BR-, IAA-, and/or GA-activated genes, including genes involved in cell wall remodeling and cell expansion. The high proportion of BR-induced genes down-regulated by *VUP1* overexpression, and an expression phenotype that at least partially mimics that of BR

Table I. *Pathway-correlated genes with significant expression alteration in VUP1 OX 9-d-old seedlings*

Arabidopsis Genome Initiative Code[a]	Probe Set	Fold Change[b]	Annotation/Name	Gene Name
At3g21710	A201725_01	16.65	VASCULAR-RELATED UNKNOWN PROTEIN1	*VUP1*
Cell wall remodeling/cell expansion related				
At2g40610	A007392_01	−3.02	Expansin, putative (EXP8)	*EXP8*
At5g06640	A025211_01	−2.79	Pro-rich extensin-like family protein	*EXT10*
At3g62680	A010954_01	−2,55	PRO-RICH PROTEIN3 (PRP3)	*PRP3*
At1g20190	A020207_01	−2.43	Expansin, putative (EXP11)	*EXP11*
At3g13520	A020452_01	−2.37	Arabinogalactan protein (AGP12)	*AGP12*
At5g56540	A022000_01	−2.29	Arabinogalactan protein (AGP14)	*AGP14*
At1g65310	A021722_01	−2.08	Xyloglucan endotransglycosylase, putative (XTH17)	*XTH17*
At4g30280	A021337_01	−2.07	Xyloglucan endotransglycosylase, putative (XTH18)	*XTH18*
At1g03870	A021074_01	−2.04	Fasciclin-like arabinogalactan protein (FLA9)	*FLA9*
At1g55330	A001679_01	−1.99	Arabinogalactan protein (AGP21)	*AGP21*
At5g49080	A025229_01	−1,92	Pro-rich protein family, EXTENSIN11	*EXT11*
At4g26320	A021004_01	−1.86	Arabinogalactan protein (AGP13)	*AGP13*
At1g69530	A020885_01	−1.84	Expansin, putative (EXP1)	*EXP1*
At4g25820	A013253_01	−1.76	Xyloglucan endotransglycosylase (XTR19, XTR14)	*XTH14*
At1g11920	A003858_01	−1.71	Polysaccharide lyase family1 (pectate lyase)	
At3g28550	A025277_01	−1.68	Pro-rich extensin-like family protein	
At3g10720	A019999_01	−1.67	Pectinesterase, putative	
At4g30290	A021957_01	−1.66	Xyloglucan endotransglycosylase (XTH19)	*XTH19*
At3g06770	A011792_01	−1.65	Polygalacturonase, putative	
At2g06850	A007964_01	−1.63	Xyloglucan endotransglycosylase, putative (XTH4)	*XTH4*
At5g09530	A020017_01	−1.61	PELPK1, PRO-RICH PROTEIN10 (PRP10)	*PRP10*
At4g30270	A024298_01	−1.58	Xyloglucan endotransglycosylase (MERI5/XTH24)	*XTH24/MERI5*
At4g38400	A014930_01	−1.58	Expansin protein family (EXPL2)	*EXPL2*
At4g08410	A024969_01	−1.54	Pro-rich extensin-like family protein	
Cell elongation related				
At3g02170	A009578_01	−1.74	LONGIFOLIA2	*LNG2*
At5g15580	A024566_01	−1.63	LONGIFOLIA1, TON1 RECRUITING MOTIF2	*LNG1, TRM2*
At2g43010	A007220_01	−1.55	PHYTOCHROME INTERACTING FACTOR4	*PIF4, SRL2*
GA and BR related				
At1g74670	A002045_01	−5.59	GA-regulated family protein	*GASA6*
At5g15230	A017092_01	−1.87	GA-regulated family protein	*GASA4*
At4g36540	A013003_01	−1.85	BRASSINOSTEROID ENHANCED EXPRESSION2 (BEE2)	*BEE2*
Auxin related				
At3g23050	A020788_01	−2.31	Auxin-responsive protein IAA7	*AXR2/IAA7*
At3g03820	A021768_01	−2.21	Auxin-induced protein, putative	*SAUR29*
At5g18010	A021410_01	−2.05	Auxin-induced protein, putative	*SAUR19*
At5g43700	A005739_01	−2.05	Auxin-responsive protein IAA4	*IAA4*
At5g18050	A021414_01	−1.99	Auxin-induced protein, putative	*SAUR22*
At5g18030	A021412_01	−1.96	Auxin-induced protein, putative	*SAUR-like*
At5g18020	A021411_01	−1.91	Auxin-induced protein, putative	*SAUR20*
At1g29430	A021746_01	−1.87	Auxin-induced protein family	*SAUR-like*
At1g04250	A020204_01	−1.84	Auxin-responsive protein IAA17	*AXR3/IAA17*
At5g18080	A021435_01	−1.84	Auxin-induced protein, putative	*SAUR24*
At1g29510	A021743_01	−1.79	Auxin-induced protein, putative	*SAUR68*
At1g29440	A021747_01	−1.74	Auxin-induced protein family	*SAUR63*
At3g03840	A021766_01	−1.67	Auxin-induced protein, putative	*SAUR27*
At1g29450	A021748_01	−1.65	Auxin-induced protein, putative	*SAUR-like*
At1g04240	A024273_01	−1.65	Auxin-responsive protein IAA3	*SHY2/IAA3*
At3g03830	A021767_01	−1.63	Auxin-induced protein, putative	*SAUR28*
At1g70940	A005209_01	−1.54	ARABIDOPSIS PIN-FORMED3 (PIN3)	*PIN3*

[a]Genes listed are summarized from Supplemental Table S1. [b]Fold change values are means of three biological replicates ($P < 0.01$).

deficiency, could explain the striking resemblance of *VUP1 OX* plants and BR-deficient mutants.

Overexpression of *VUP1* Inhibits BR- and Light-Dependent Signaling

The down-regulation of BR- and GA-activated genes in *VUP1 OX* transgenic plants could be the consequence of reduced BR or GA biosynthesis or increased degradation. Thus, we first tested whether exogenously applied brassinolide (BL; the biologically most active BR) or GA_3 could rescue the growth defects of *VUP1 OX* plants. Topical application of BL or GA_3 or supplementing growth media with BL and/or GA_3 had little or no effect on *VUP1 OX* seedling growth (Fig. 8A),

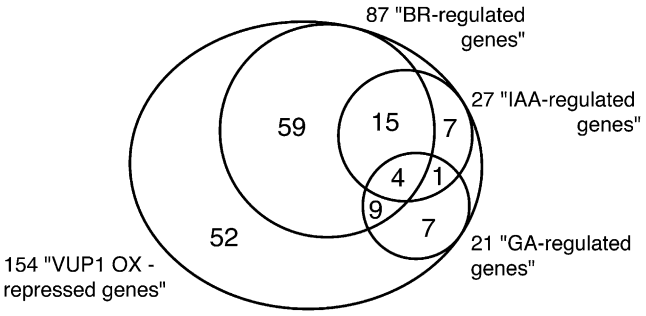

Figure 7. Relative proportion of *VUP1 OX* down-regulated genes that are coregulated by BR, IAA, and GA. The Venn diagram shows the number of genes down-regulated in *VUP1 OX* seedlings that are also regulated by BR, IAA, and/or GA. Lists of BR-, IAA-, and GA-regulated genes are from previously published microarray data sets: BR (Sun et al., 2010), IAA (Goda et al., 2004, 2008), and GA (Cao et al., 2006).

indicating that *VUP1 OX*-induced dwarfism is not the consequence of a reduced availability of biologically active BR or GA. Furthermore, these results indicate that *VUP1 OX* plants are at least partially insensitive to BR and GA.

Next, we investigated whether *VUP1* ectopic expression inhibits GA or BR signaling pathways. A current model for the regulatory network governing seedling growth and hypocotyl elongation that integrates BR, GA, and light signaling pathways is shown in Figure 8B. These pathways converge at the level of the BRASSINAZOLE RESISTANT (BZR)-DELLA-PIF transcription module to regulate the expression of a large number of genes that contribute to elongation growth and other BR-, GA- and/or light-dependent responses (Sun et al., 2010; Bai et al., 2012b; Gallego-Bartolomé et al., 2012; Jaillais and Vert, 2012; Oh et al., 2012). To test a potential role of VUP1 in this regulatory network, we used gain- and loss-of-function mutants of signaling components, exhibiting an increased and/or constitutive BR signaling for BR pathway (*bri1-ems suppressor1-1D* [*bes1-1D*] and *bzr1-1D*) and GA pathway (*penta*) signaling or a decreased phytochrome-mediated signaling (*PhyB-1*; Fig. 8B, gray labels). We transformed these mutants with the *VUP1 OX* construct (*pro35S*:*VUP1*:*YFP*), and the phenotypes of seedlings overexpressing *VUP1* in the mutant backgrounds were assessed to infer the epistatic genetic interactions of *VUP1* with these known regulators.

GA promotes growth via a signaling pathway that leads to the degradation of growth-repressing DELLA proteins (Sun, 2011). The *penta* pentuple mutant combines loss-of-function alleles of all five members of the Arabidopsis *DELLA* family and exhibits constitutive GA signaling. Phenotypic analysis of *pro35S*:*VUP1 penta* seedlings revealed a growth inhibition phenotype similar to *VUP1 OX* (wild-type background; Fig. 8C), indicating that VUP1 inhibits elongation growth independently from DELLAs and upstream GA signaling components.

The two gain-of-function mutants *bzr1-1D* and *bes1-1D* have elevated active BZR1 and BES1 (also called BZR2) transcription factors (Wang et al., 2002; Yin et al., 2002), resulting in constitutive and BR-independent activation of the BR signaling pathway. *bes1-1D* seedlings exhibit consistent pale green enlarged leaves and abnormally elongated hypocotyls and petioles (Fig. 8C). Overexpression of *VUP1* in these two genetic backgrounds (*pro35S*:*VUP1 bzr1-1D* and *pro35S*:*VUP1 bes1-1D*) resulted in seedlings phenotypically similar to *VUP1 OX* (wild-type background), indicating than *VUP1*-induced growth inhibition is independent of components upstream of BZR1 and BES1. Interestingly, the characteristic increased elongation growth of *bes1-1D* was not observed in *pro35S*:*VUP1 bes1-1D* plants, suggesting that *VUP1* overexpression inhibits a BES1-dependent signaling pathway at the level or downstream of BES1/BZR1.

The *PHYB* loss-of-function mutant *PhyB-1* has a partially constitutive etiolated phenotype, an abnormally long hypocotyl, light green color, greater apical dominance, and abnormally elongated petioles and stems, pleiotropic phenotypes that are the result of altered phytochrome-mediated light signaling (Reed et al., 1994; Fig. 8). Overexpression of *VUP1* in the *PhyB-1* mutant background (*PhyB-1 pro35S*:*VUP1*) resulted in severe dwarfism similar to that of *VUP1 OX* in wild-type plants (Fig. 8C), indicating a light/*PHYB*-independent growth inhibition by *VUP1*. Interestingly, as for *bes1-1D*, the constitutive etiolation and increased elongation growth that are hallmarks of *PhyB-1* seedlings were not observed when *VUP1* was overexpressed in this background, indicating that *VUP1* overexpression inhibits downstream components of the PHYB-dependent, as well as BES1-dependent, signaling pathways that promote elongation growth. Altogether, our results suggest a dominant inhibitory effect of VUP1 at the level of, or downstream of, the BZR-DELLA-PIF transcription module. This is consistent with the down-regulation of a large number of "BR-regulated" or "BZR1-regulated" genes in *VUP1 OX* seedlings.

Overexpression of VUP1 Subdomains M1 to M3 Is Sufficient and Necessary for the *VUP1 OX*-Induced Growth Inhibition

VUP1 is a small protein that shares low overall sequence conservation with VUP1 homologs, except in four short highly conserved domains of nine to 20 residues (M1–M4; Fig. 2). To query their roles in *VUP1 OX*-induced growth inhibition and VUP1 function, we created a set of truncated *VUP1* constructs encoding proteins that lack one or several conserved domains (Fig. 9A). These truncated *VUP1* derivatives were fused to the *YFP* gene and overexpressed in Arabidopsis. YFP-derived fluorescence was verified for all lines analyzed, and the impacts on plant development were analyzed in T1 and T2 generations. Overexpression of the $VUP1^{1-165}$ and $VUP1^{1-126}$ versions, lacking M4 with or without the adjacent non-conserved sequence (Fig. 9A), led to similar phenotypes to full-length *VUP1* overexpression: dwarf, dark green plants with reduced etiolated seedling hypocotyl lengths

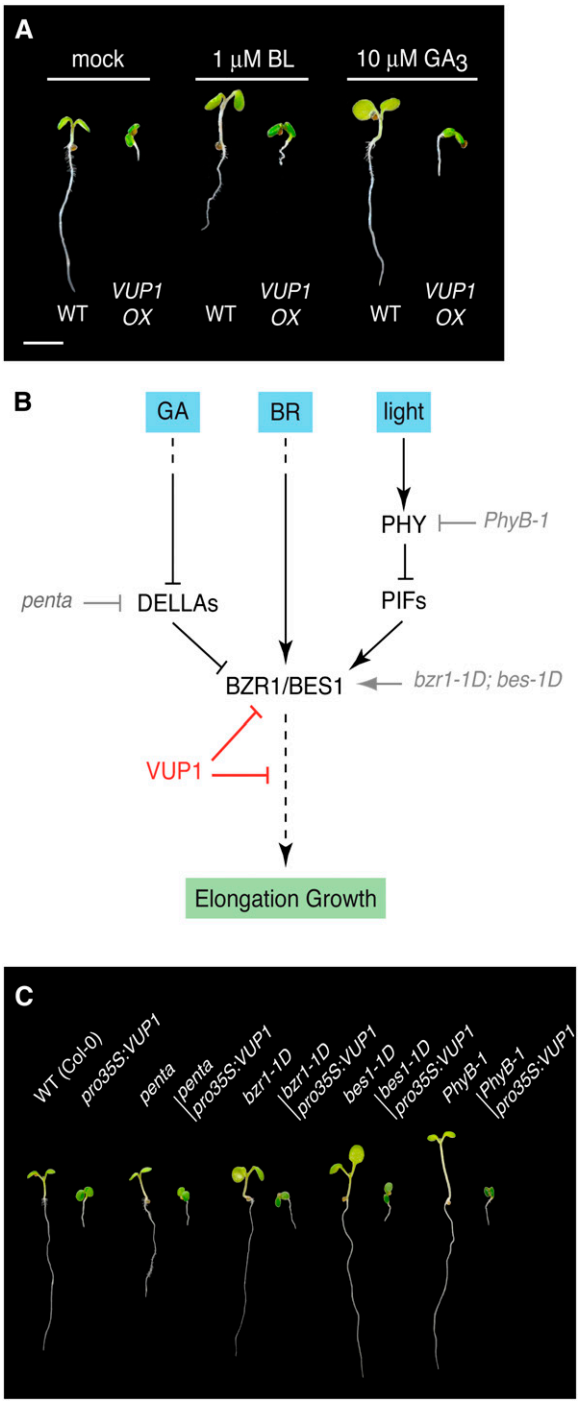

Figure 8. Genetic interaction between *VUP1* and various mutants with altered photomorphogenic growth. A, Phenotypes of representative 7-d-old wild-type (WT) and *VUP1 OX* T2 seedlings grown on one-half-strength MS medium not supplemented or supplemented with 1 μM BL or 10 μM GA_3. B, Simplified model for the signaling network integrating BR, GA, and light signals. BZR1 and BES1 regulate a large number of genes that contribute to hypocotyl elongation. PIF4 forms a functional complex with BZR1 to promote elongation growth. DELLAs interact with BZR1 and PIFs to inhibit their DNA-binding ability. BR, GA, and light/phytochrome signals modulate the level of active BZR1/BES1, DELLAs, and PIFs, respectively, thereby controlling seedling elongation growth. Gray arrows and bar-headed lines represent the action of gain- and loss-of-function mutants (named in gray) that activate or inhibit the corresponding signaling pathways. In red, the potential inhibitory action of VUP1 on elongation growth, at the level or downstream of BZR1/BES1, is shown. C, Phenotypes of representative 7-d-old light-grown wild type, *VUP1 OX* T2, *penta*, *bzr1-1D*, *bes1-1D*, *PhyB-1*, and mutants transformed with a *VUP1 OX* construct (*VUP1 OX penta*, *VUP1 OX bzr1-1D*, *VUP1 OX bes1-1D*, and *VUP1 OX PhyB-1*).

(Fig. 9B), although the $VUP1^{1\text{-}126}$ overexpression phenotype was weaker and intermediate between those of etiolated *VUP1 OX* and wild-type seedlings (Fig. 9B). Similarly, overexpression of the minor splice variant *VUP1.1*, which encodes a protein sharing the first 150 amino acids with the major splice variant *VUP1.2*, led to a phenotype indistinguishable from *VUP1* full-length overexpression (Fig. 9B). These results indicate that M4, and more generally the last 85 residues of VUP1, are not necessary for VUP1 growth inhibitory activity. Consistent with this, overexpressors of the truncated version $VUP1^{186\text{-}211}$ (Fig. 9A) were also phenotypically similar to the wild type (Fig. 9). Conversely, plants overexpressing truncated versions lacking M1, M2, and/or M3 ($VUP1^{80\text{-}211}$, $VUP1^{1\text{-}94}$, and $VUP1^{1\text{-}71}$) exhibited no developmental defects and were phenotypically similar to the wild type (Fig. 9B), demonstrating that a core VUP1 region including conserved domains M1, M2, and M3 is necessary and sufficient for *VUP1 OX*-induced growth defects.

Site-Directed Mutagenesis Defines Important Residues for VUP1 Function

To further explore the VUP1 structural basis of the *VUP1 OX*-induced growth inhibition, we targeted highly conserved residues in domains M1, M2, or M3 for substitution with Ala, singly or in pairs when two adjacent amino acid residues were identical or similar (Fig. 10A). These *VUP1* variants were expressed as C-terminal translational fusions with a hemagglutinin (HA)-tagged YFP and placed under the control of the 35S promoter [*pro35S*:$VUP1^{mut}$:*YFP(HA)*] and transformed into Arabidopsis.

Analysis of seven different *pro35S*:$VUP1^{mut}$:*YFP(HA)* variants ($VUP1^{E36A;\ E37A}$, $VUP1^{S38A}$, $VUP1^{Y43A}$, $VUP1^{S78A}$, $VUP1^{D79A}$, $VUP1^{S120A}$, and $VUP1^{P121A}$) revealed no obvious differences in comparison with the overexpression of wild-type *VUP1*, displaying typical severe dwarfism, dark green leaves, and reduced hypocotyl lengths (Fig. 10, B and C). Interestingly, the mutated version $VUP1^{T117A}$ exhibited an enhanced phenotype with smaller leaves and reduced rosette size (Fig. 11B) and a very short stem with no or few seeds (data not shown). Because of its low fertility, $VUP1^{T117A}$ overexpression could not be analyzed at the T2 generation. Conversely, overexpression of two variants ($VUP1^{W40A}$ and $VUP1^{E115A;\ D116A}$) resulted in phenotypically normal

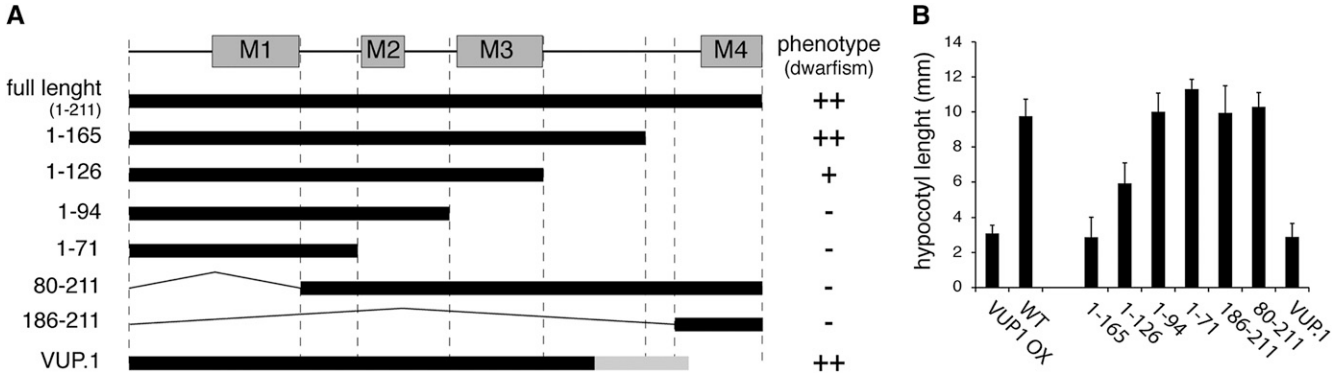

Figure 9. Phenotypic analysis of seedlings overexpressing truncated *VUP1* versions. A, Schematic diagram representing the partial sequences of VUP1 (thick black lines) used for overexpression. The top shows the conservation of corresponding amino acid sequences. Gray boxes represent the conserved motifs M1 to M4. *VUP1.1* is the *VUP1* alternative splice variant sharing the first 150 amino acids with *VUP1* and with a different 25 amino acids at the C terminus (thick gray line). At right, the severity of the phenotype induced by the overexpression of the corresponding truncated version based on qualitative observation of 4-week-old plants, representative of five or more independent lines, is shown: ++ indicates a strong dwarfism similar to that observed for *VUP1 OX* plants; − indicates no growth defects relative to the wild type; and + indicates an intermediate phenotype between wild-type and *VUP1 OX* plants. B, Hypocotyl lengths of 5-d-old etiolated seedlings for the wild type (WT) and overexpressors of *VUP1* truncated versions. Two independent lines for each construct were used for phenotypic quantification ($n > 10$).

plants without apparent growth inhibition or chlorophyll hyperaccumulation (Fig. 10B). Overexpression of $VUP1^{S119A;\ S120A}$ resulted in slight dwarfism at the seedling stage, which, however, was not apparent in rosette-stage plants relative to the wild type (data not shown), while overexpression of the variant $VUP1^{T41A;\ T42A}$ led to an intermediate dwarf phenotype (Fig. 10, B and C).

In order to verify that the altered phenotypes conditioned by overexpression of these VUP1 variants was not due to enhanced protein degradation, the HA-tagged variant proteins were analyzed by western blotting. No significant differences in VUP1 variant protein accumulation relative to wild-type VUP1 were observed (Supplemental Fig. S5). Furthermore, confocal microscopy did not reveal differences in the subcellular localization of the corresponding YFP-tagged proteins relative to the wild type (data not shown). These results identify Trp-40, Glu-115/Asp-116, and Ser-119/Ser-120 as critical residues for VUP1-induced growth inhibition. As they do not appear to be involved in protein trafficking or stability, these residues are likely necessary for VUP1 cellular function. Interestingly these critical residues are among the few that are strictly conserved among all VUP1 homologs in Arabidopsis and other tracheophytes (Figs. 2B and 10B), suggesting a common mode of action for the VUP1 protein family and supporting the idea of a conserved mechanism of growth regulation.

VUP1 Phosphorylation Regulates Its Activity

Examination of the VUP1 sequence revealed Ser or Thr residues in the correct context to be potential phosphoacceptors, including conserved Ser residues Ser-120 and Ser-124 and Thr residue Thr-117 in motif M3 (Figs. 2B and 11A). To assess whether phosphorylation could participate in the regulation of VUP1 activity, we queried the PhosPhAt 4.0 database (Durek et al., 2010) and found a reported phospho-VUP1 version (a double phosphorylation on Ser-120 and Ser-124; Fig. 11A) in a large-scale phosphoproteomic experiment (Wang et al., 2013). Because Ser-120 is strictly conserved in VUP1 homologs, in contrast with the partial conservation of Ser-124, we further investigated the function of putative phosphorylation at this position. As discussed above, S120A mutation did not affect the *VUP1* overexpression phenotype, suggesting that Ser-120 phosphorylation is not necessary for this aspect of VUP1 function (Fig. 10). We next tested the effect of a Ser-120 substitution by an Asp residue (S120D) that mimics a constitutive phosphorylation at this position. This $VUP1^{S120D}$ phosphomimic mutation fully suppressed the *VUP1 OX* phenotype (Fig. 11), suggesting that phosphorylation of Ser-120 results in inactive VUP1.

Intriguingly, overexpression of a T117A substitution ($VUP1^{T117A}$ *OX*) resulted in a stronger phenotype than *VUP1 OX* (Fig. 11), suggesting enhanced VUP1 activity in the mutant. To test whether putative phosphorylation on Thr-117 affects VUP1 activity, we produced the Thr-117 phosphomimetic version ($VUP1^{T117D}$). The *VUP1 OX* phenotype was also strongly suppressed in $VUP1^{T117D}$-overexpressing plants, although the plants still exhibited a mild dwarf phenotype (Fig. 11).

In order to determine whether phosphorylation of Ser-120 and Thr-117 triggered increased VUP1 degradation, the HA-tagged variant proteins were analyzed by western blotting. No significant differences in VUP1 variant protein accumulation relative to wild-type VUP1 were observed (Supplemental Fig. S5). Taken together,

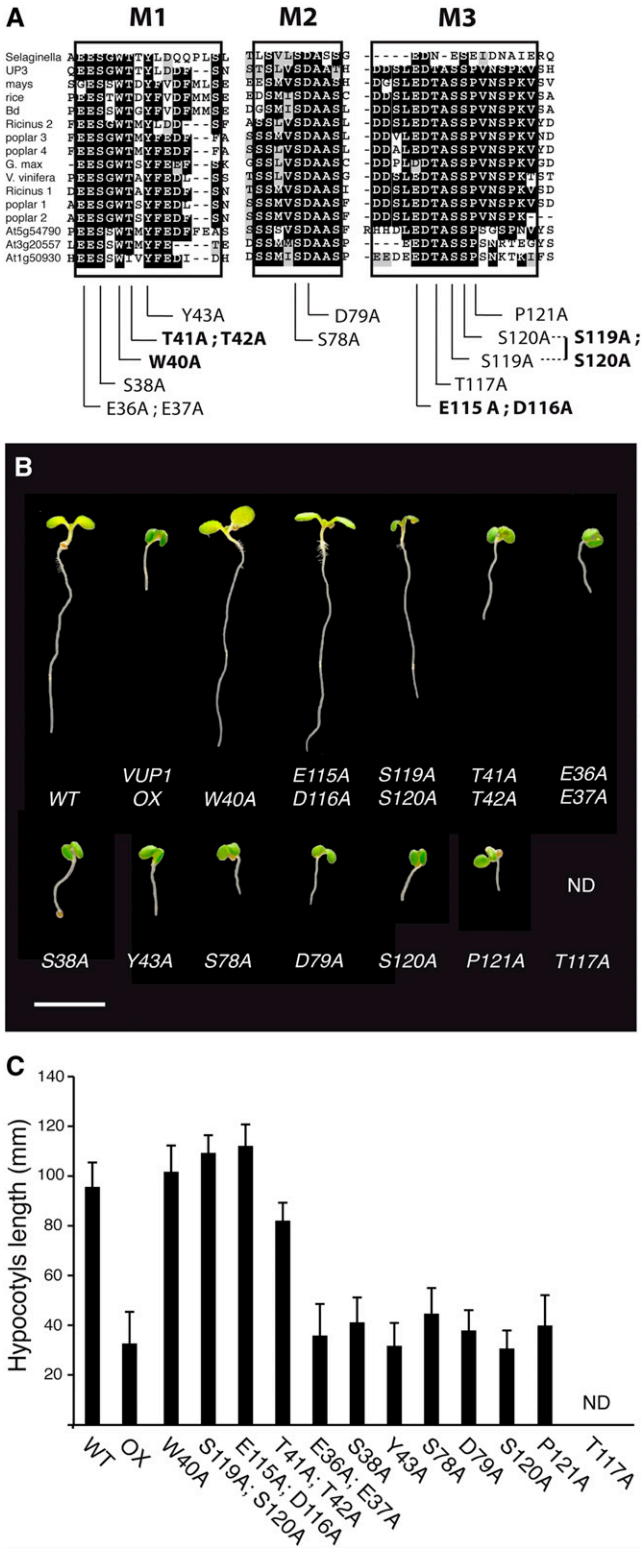

Figure 10. Point mutations in the *VUP1* sequence affect the *VUP1 OX* phenotype. A, Partial views of an alignment of VUP1 and selected homologs showing the conserved regions M1, M2, and M3. The substitutions resulting from site-directed mutagenesis described in the text are indicated below. The substitutions leading to total or partial reversion of the *VUP1 OX* phenotype are indicated in boldface. B, Representative phenotypes of the wild type (WT) and overexpressors of wild-type and mutated *VUP1* versions in 7-d-old seedlings (T2). The results are representative of five or more independent lines analyzed. ND, No data. Bar = 0.5 cm. C, Five-day-old etiolated seedling hypocotyl lengths of the wild type and overexpressors of wild-type and mutated *VUP1* versions. Two independent lines for each version were chosen for quantitative analysis ($n > 10$).

these results indicate that phosphorylation of Thr-117 and Ser-120 participates in the regulation of VUP1 activity, with nonphosphorylated VUP1 being highly active while phospho-VUP1 has greatly reduced activity.

Overexpression of *VUP1* Homologs from Various Vascular Plants Phenocopies *VUP1 OX* Plants

The high conservation of motifs M1 to M3 in VUP1 homologs in Arabidopsis and other tracheophyte species (Fig. 2B) raises the possibility of functional conservation. To address this question, sequences of seven homologs from eudicots (three Arabidopsis and four poplar [*Populus trichocarpa*]), one homolog from the monocot *Brachypodium distachyon*, and one homolog from the more divergent lycophyte *S. moellendorffii* were overexpressed in Arabidopsis under the control of the 35S promoter. Overexpression of the three Arabidopsis homologs, *VUP2* (*At1g50930*), *VUP3* (*At3g20557*), and *VUP4* (*At5g54790*; sharing 38.2%, 30.9%, and 39.6% amino acid similarity with VUP1, respectively), led to phenotypes indistinguishable from *VUP1 OX* lines, severely dwarf plants (Fig. 12).

The four poplar (*P. trichocarpa* version 2.2) *VUP1* homologs (*POPTR_0002s23090*, *POPTR_0014s15000*, *POPTR_0001s44530*, and *POPTR_0011s13900*) share 47.3%, 46.4%, 46.1%, and 45.5% amino acid similarity with VUP1, respectively. Their overexpression in Arabidopsis likewise resulted in severe growth inhibition similar to *VUP1 OX* lines, but with some differences. As illustrated in Figure 12, overexpression of *POPTR_0002s23090* resulted in a high density of root hairs, while root growth inhibition was not as severe in comparison with shoot inhibition in *POPTR_0014s15000 OX* lines. Similarly, overexpression of the *B. distachyon* homolog (*BdVUP1*, *Bradi1g25990*; 39% amino acid similarity with VUP1) induced growth defects indistinguishable from *VUP1 OX* plants (Fig. 12C). Interestingly, overexpression of the divergent *S. moellendorffii* homolog (*SmVUP1*, fgenesh2_pg.C_scaffold_9000114; 35.3% amino acid similarity with VUP1), which shows a particularly low sequence conservation in the conserved motifs (Fig. 2A), led to a similar but even stronger phenotype in comparison with *VUP1 OX* (Fig. 12, D and E). Most of the *S. moellendorffii VUP1* overexpressors died quickly after germination, and none of the eight T1 plants grew larger than 5 mm in diameter or produced seeds, in contrast to *VUP1 OX* or other homolog overexpression lines (data not shown).

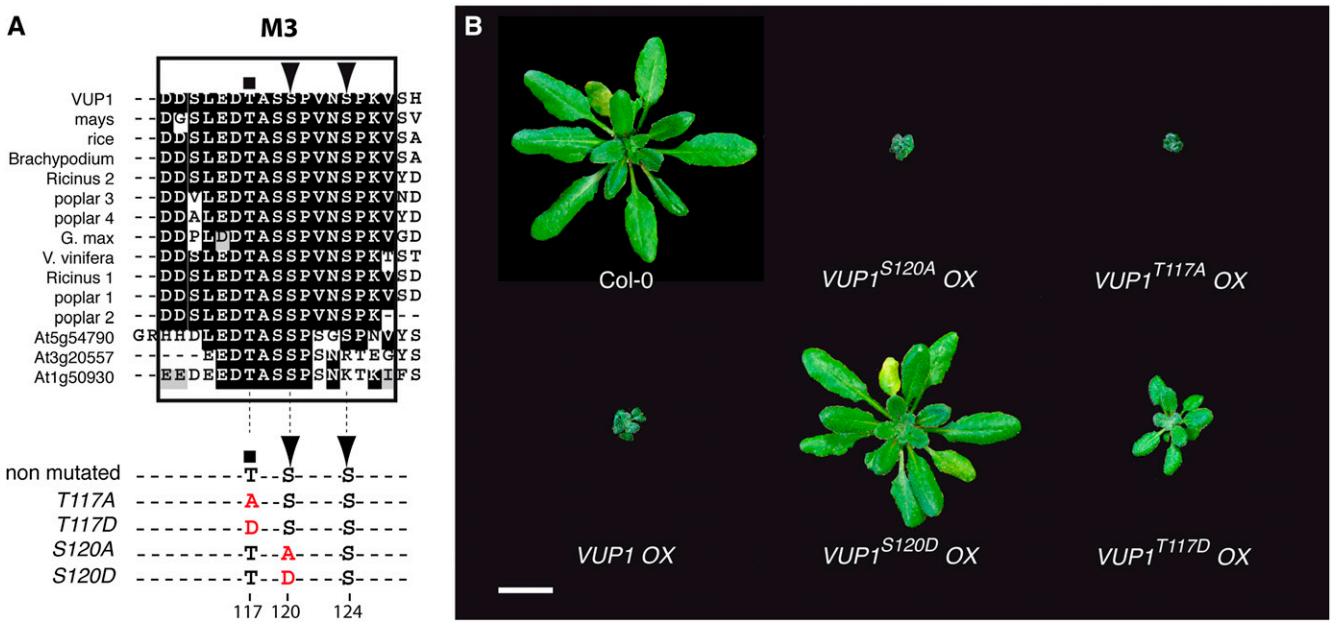

Figure 11. Effects of phosphomimetic substitutions in the VUP1 sequence. A, Partial view of an alignment of VUP1 and selected homologs showing the conserved region M3. The experimentally determined (Wang et al., 2013) phosphorylation sites are indicated by arrowheads. A putative phosphoacceptor residue is indicated by the square. Phosphonull and phosphomimetic substitutions described in the text are indicated below. B, Representative phenotypes of 4-week-old plants of the wild type, *VUP1 OX*, and overexpressors of phosphonull and phosphomimetic versions of *VUP1*. The phenotypes shown are representative of at least three independent lines. Bar = 1 cm.

Thus, despite low overall sequence conservation, very similar defects were induced by the overexpression of *VUP1* and *VUP1* homologs from various tracheophyte species. This supports the idea of a functional conservation of VUP1 proteins among tracheophytes, mediated by key conserved protein domains containing a few critical residues. Consistent with this, the crucial residues revealed by site-directed mutagenesis of *VUP1* are all found in these homologs, including the *S. moellendorffii* homolog.

DISCUSSION

Conservation of VUP1 Protein Structure Overexpression Phenotypes Implies Important Functions

The *VUP1* gene family in Arabidopsis and putative orthologs in other tracheophytes encode predicted novel proteins containing no previously characterized domains or motifs. *VUP1* and *VUP1* homologs are strictly conserved among vascular plants, suggesting that they perform important and conserved roles in plant development and/or physiology in this lineage. We show that *VUP1* homologs share highly conserved motifs (M1–M4) that, with the exception of M4, are essential for VUP1 function. With the exception of M4, these conserved motifs are not present in any other proteins in the databases and seem specific to this gene family. As such, they represent signature sequences for VUP1-like proteins, and although of still uncharacterized molecular function, we show that they are critical for VUP1 biological function in regulating hormone and light-mediated elongation growth. In support of a common, conserved VUP1 function in tracheophytes, the overexpression of all *VUP1* homologs from poplar, *B. distachyon*, and *S. moellendorffii* in Arabidopsis gave similar phenotypes as *VUP1* overexpression (Fig. 12).

Elucidation of *VUP1* molecular function by employing loss-of-function approaches in Arabidopsis may be limited by functional redundancy with three other Arabidopsis *VUP1-like* (*VUP2–VUP4*) putative paralogs. In support of this, *VUP2* to *VUP4* contain all of the motifs and residues shown to be essential for VUP1 function (Figs. 2, 8, and 9), and their overexpression results in defects in growth and development very similar to those observed for *VUP1 OX* plants (Fig. 12). Microarray-based expression profiles indicate that Arabidopsis *VUP1* homologs are weakly expressed throughout plant organs and developmental stages, with higher expression in the roots for *VUP2* and *VUP4* (AtGenExpress, TileViz). In addition, RT-PCR analysis showed that the expression of all three *VUP1* homologs is detectable in stems (E. Grienenbeger, unpublished data). Therefore, it is plausible that *VUP1* homologs have partially overlapping molecular functions and expression patterns and can thus, at least partially, complement each other's functions. This may explain the rather mild *irx* phenotype observed in *vup1* loss-of-function mutants relative to the strong phenotypic effects conditioned by *VUP1* overexpression. Further testing of possible redundant *VUP* gene functions

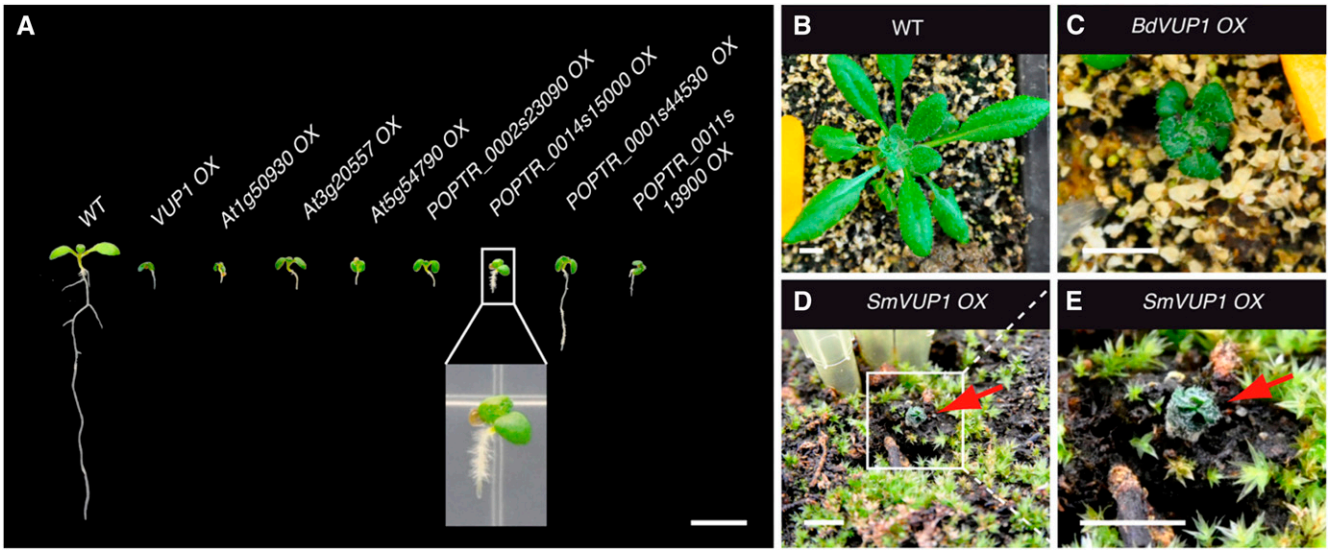

Figure 12. Consequences of the overexpression of *VUP1* homologs in Arabidopsis. A, Representative phenotypes of 10-d-old Arabidopsis seedlings overexpressing *VUP1* and the three Arabidopsis and four poplar *VUP1* homologs. A 10-d-old wild-type (Col-0) plant (WT) is shown as a control. B and C, Three-week-old wild-type (B) and *B. distachyon VUP1* homolog-overexpressing (*BdVUP1*; Bradi1g25990) plants (C). D and E, An 8-week-old *S. moellendorffii VUP1* homolog-overexpressing plant (*SmVUP1*; fgenesh2_pg.C_scaffold_50000023). Arrows indicate rosette leaves of the *SmVUP1* overexpressor. More than five independent transformants were analyzed for all overexpressors except for *SmVUP1 OX*, where three transformants were analyzed. Bars = 1 cm.

will require analysis of higher order *VUP* loss-of-function mutant combinations. While we identified T-DNA insertion mutants in *VUP2*, *VUP3*, and *VUP4* and were able to generate *vup1 vup2 vup4* as well as *vup2 vup3 vup4* triple mutants (E. Grienenberger, R. Yoon, and C. Douglas, unpublished data), tight linkage between *VUP1* and *VUP3* precluded generation of the *vup1 vup3* mutant combination. None of the triple mutants showed obvious growth or other additional phenotypes relative to wild-type plants (E. Grienenberger, R. Yoon, and C. Douglas, unpublished data).

Our work shows that *VUP1* and its encoded protein are subject to multiple levels of regulation. *VUP1* expression is restricted to specific cells and tissues, VUP1 is rapidly turned over when overexpressed, and VUP1 phosphorylation is critical for the regulation of its activity. The combination of phosphoregulation and rapid protein turnover suggests that a tight control of VUP1 levels and activity is crucial for normal plant development, consistent with the strong deleterious pleiotropic effects induced by *VUP1* misexpression.

VUP1 biological function is most evident in plants that misexpress *VUP1*, and this activity requires specific VUP1 domains and sequences. Indeed, single substitutions in conserved VUP1 amino acid residues resulted in complete loss of pleiotropic growth defects. Furthermore, site-directed mutagenesis, overexpression of truncated *VUP1* versions, and overexpression of *VUP1* homologs clearly demonstrated that *VUP1 OX*-induced defects are dependent on a few highly conserved residues in the VUP1 protein. This specific structure-function relationship supports the idea that a highly specific molecular mechanism leads to *VUP OX*-induced defects.

Overexpression of *VUP1* Interferes with Hormone Signaling Pathways

The reduced apical dominance, late flowering, altered skotomorphogenesis, as well as the severe dwarfism and reduced cell expansion phenotypes conditioned by constitutive overexpression of *VUP1* are suggestive of defects in hormone responses (Bishop and Koncz, 2002; Gazzarrini and McCourt, 2003; Hu and Ma, 2006). Cell expansion and plant morphogenesis are controlled by light and hormones such as BR, GA, and auxin (Rymen and Sugimoto, 2012). It has been recently proposed that light, BR, and GA act interdependently to control key growth processes (Bai et al., 2012b; Jaillais and Vert, 2012; Oh et al., 2012) and that these signaling pathways are integrated through the transcription factors BZR1 and BZR2/BES1 (Kim and Wang, 2010) as well as through DELLA repressors and PIF transcription factors (Bai et al., 2012b; Fig. 8B).

VUP1 OX seedlings closely resemble BR- and GA-deficient or -insensitive mutants, sharing in common a dwarf stature, altered morphogenesis, and dark green leaves. Growth inhibition associated with BR signaling is consistent with our transcriptome profiling of *VUP1 OX* seedlings: among the genes down-regulated relative to wild-type seedlings, 56% have been shown to be BR regulated in various studies, including genes encoding expansins, *XTHs*, or other facilitators of cell wall expansion

(Sun et al., 2010; Bai et al., 2012b). Furthermore, the expansin genes *EXP8* and *EXP1*, which were among those that exhibited the highest negative fold change in *VUP1 OX* seedlings (Table I), are the direct targets of the BZR1/PIF4 heterodimer (Bai et al., 2012b) as well as of the BR/BZR1-activated HOMOLOG OF BEE2 INTERACTING WITH IBH1 (Bai et al., 2012a). Expression profiling of *VUP1 OX* seedlings also suggests a possible involvement of *VUP1* in auxin (IAA) and GA signaling, based on the relatively large number of GA- and IAA-related genes among the 154 significantly down-regulated genes in *VUP1 OX* seedlings (Fig. 7).

Exogenously applied BL and/or GA_3 did not rescue *VUP1 OX* dwarfism (Fig. 8A), indicating that a reduced level of these hormones is not the cause of the altered growth and that these plants are BR and GA insensitive. This suggests that BR- and GA-dependent signaling is blocked by VUP1 misexpression. Overexpression of *VUP1* in different genetic backgrounds exhibiting constitutive BR, GA, or light/phytochrome signaling (*bzr1-1D*, *bes1-1D*, and *PhyB-1*) did not result in a reversion of the phenotype; however, the enhanced growth promoted by the stabilization of BES1 in the *bes1-1D* gain-of-function mutant and the partial constitutive etiolation observed in the *PhyB-1* mutant were clearly absent upon concomitant *VUP1* overexpression, suggesting that VUP1 acts at the level of, or downstream of, the integration of these signaling pathways by BZR1/BES1 transcription factors (summarized in Fig. 8B). Taken together, our data are most consistent with a profound negative effect of VUP1 on the combined effects of BR, GA, and light signaling late in these pathways, most likely after their convergence, as summarized in Figure 8B.

Possible Mechanisms of VUP Action

Despite our extensive structure-function analysis, the mechanism by which VUP1 and other VUP proteins could inhibit BR, GA, and light signaling remains unclear. The pleiotropic effects resulting from its misexpression combined with expression and genetic data favor a regulatory role for VUP1. However, the nature of its putative regulatory function is unclear, since its subcellular localization is ambiguous (nuclear and/or cytoplasmic) and neither a DNA-binding domain nor transcriptional activation or repression domains are predicted. We assayed the ability of VUP1 to activate or repress transcription protoplasts in transient assays but were unable to detect any activity (E. Grienenberger, unpublished data), while plants expressing *VUP1* fused to the transcriptional repressor domain SRDX (*pro35S*:*VUP1*:*SRDX*) had similar defects to *VUP1 OX* plants (data not shown). Therefore, it does not appear that VUP1 alone has transcriptional activation activity. It is possible, however, that VUP1 acts as part of a transcriptional complex and requires partner components for its activity. Finally, it is possible that VUP1 is involved in other modes of regulation, such as participating in one or more signal transduction pathways or modulating protein trafficking.

One possibility is that VUP1 antagonizes the action of one or more transcription factors by interacting with them, analogous to non-DNA-binding atypical bHLH transcriptional regulators. These small proteins lack DNA-binding domains but dimerize with DNA-binding bHLH proteins to inhibit DNA binding (Ruzinova and Benezra, 2003; Zhang et al., 2009) or interact with other atypical bHLHs to antagonize their action (Bai et al., 2012a; Ikeda et al., 2012). Examples include PACLOBUTRAZOL RESISTANCE1 (PRE1) and PRE6/KIDARI, which positively regulate organ elongation in response to GA, BR, and light signaling (Hyun and Lee, 2006; Lee et al., 2006a; Wang et al., 2009) by their interaction with the bHLH negatively acting transcription factors ACTIVATION-TAGGED bri1 SUPRESSOR1 (ATBS1)-interacting factors and LONG HYPOCOTYL IN FAR-RED1. Potential protein interaction partners of VUP1, however, remain to be demonstrated. Indeed, no interactors for VUP1 and its Arabidopsis homologs could be found in the Plant Interactome Database (Arabidopsis Interactome Mapping Consortium, 2011). Furthermore, we were unable to identify any interacting partners in a yeast two-hybrid screen using VUP1 as bait (E. Grienenbeger, unpublished data). It is possible, however, that a posttranslational modification that does not occur in yeast is required for VUP1 interacting ability. It is also possible that a third protein is required. In this context, coimmunoprecipitation experiments to identify possible protein complexes that contain VUP1 might be particularly informative.

Several lines of evidence suggest that VUP1 might directly inhibit BZR1. We found that the expression of two BZR1 direct targets (*EXP1* and *EXP8*; Bai et al., 2012b) is strongly reduced in *VUP1 OX* seedlings. Additionally, of the 154 *VUP1 OX* down-regulated genes, 36% (56 of 154) are putative BZR1 direct targets, as defined by Sun et al. (2010) in a chromatin immunoprecipitation/microarray hybridization experiment, whereas the probability of randomly affecting a BZR1 target gene would be about 11%. Since the *bzr1-1D* gain-of-function mutation does not rescue the phenotype induced by *VUP1* overexpression, VUP1-dependent inhibition of BR signaling is likely to occur at the level of, or downstream of, BZR1. Inhibition at the level of this master regulator is indeed in good agreement with the strong and pleiotropic effects observed in *VUP1 OX* plants.

Possible Specific Functions for VUP1

The vascular-related *VUP1* expression pattern together with the *irx* phenotype observed in the *vup1* mutants indicate a function of *VUP1* in xylem differentiation and/or secondary wall formation, while *VUP1* overexpression suggests a role in regulating BR- and/or GA-dependent signaling. A possible explanation for these observations is that *VUP1* functions in vascular development/secondary wall formation by modulating hormone signaling pathways in a cell- or tissue-specific manner. There is good

evidence for the involvement of BRs and GAs in xylem differentiation. For example, BR-deficient Arabidopsis mutants are extreme dwarfs with reduced amounts of xylem (Szekeres et al., 1996; Choe et al., 1999; Milhinhos and Miguel, 2013). The application of brassinazole, a specific inhibitor of BR biosynthesis, to Arabidopsis seedlings causes reduced xylem formation (Nagata et al., 2001), while BL promotes xylogenesis in *Z. elegans* and Arabidopsis cell culture (Yamamoto et al., 1997, 2001; Yamaguchi et al., 2010). Recent findings also suggest that GA is the mobile shoot-derived signal that triggers xylem expansion upon flowering initiation in Arabidopsis and tobacco (*Nicotiana tabacum*; Ragni et al., 2011; Dayan et al., 2012).

While endogenously produced BRs and GAs can evidently promote xylem differentiation, the nature of the BR- or GA-dependent signaling underlying xylogenesis remains largely unknown. It has been proposed that BR, through a BZR1-dependent signaling pathway, promotes xylem differentiation by increasing the expression of *HD-Zip III* genes involved in vascular patterning (Ohashi-Ito et al., 2002; Ohashi-Ito and Fukuda, 2003; Cano-Delgado et al., 2004; Fukuda, 2004). In *Z. elegans* xylogenic cells, BR depletion severely suppresses the expression of the three *HD-Zip III* genes *ZeHB10*, *ZeHB11*, and *ZeHB12* (*AtHB8* and *REV* Arabidopsis homologs) in xylem precursor cells and differentiating xylem cells (Ohashi-Ito et al., 2002; Ohashi-Ito and Fukuda, 2003), and the three genes are induced within 1 h by BL in *Z. elegans* cells, indicating that they respond rapidly to BRs (Ohashi-Ito and Fukuda, 2003). Therefore, BR might regulate differentiation from procambium to xylem through the expression of specific members of the *HD-ZIP-III* family, and it is possible that VUP1 regulates their expression through a BR-dependent signaling pathway, possibly by modulating BZR1 activity as discussed above. Interestingly the poplar *VUP* homolog most similar to Arabidopsis *VUP1*, *POPTR_0011s13900*, is expressed in developing poplar secondary xylem (Bao et al., 2013) and shows a highly xylem-preferred expression pattern (C. Hefer, C. Douglas, and S. Mansfield, unpublished data), consistent with a role for poplar VUP1 in secondary xylem differentiation. Further studies of VUP1 and its homologs, as well as possible interacting proteins, should yield new insights into the mechanisms by which BR, GA, and light signaling pathways control cell expansion growth, vascular differentiation, and other aspects of plant morphogenesis.

MATERIALS AND METHODS

Plant Materials and Growth Conditions

Arabidopsis (*Arabidopsis thaliana*) plants were of the Columbia (Col-0) wild-type ecotype. Seedlings and plants were grown under long-day conditions (16 h of light/8 h of dark) at 22°C. Seeds were surface sterilized with 70% (v/v) ethanol for 10 to 15 min and placed on one-half-strength Murashige and Skoog (MS) medium with 1% (w/v) Suc and 0.7% (w/v) agar. Seeds were stratified for 2 or 3 d at 4°C in darkness before being placed vertically in a growth chamber equipped with fluorescent white light (light intensity of 70–120 μmol m^{-2} s^{-1}). For *proVUP:VUP1:GUS* plants, seedlings were selected on one-half-strength MS medium with 25 μg mL^{-1} hygromycin. For dark conditions, plates were wrapped in several layers of aluminum foil. Growth days were counted from when the plate was placed in the growth chamber. For hormonal tests, seedlings were grown in one-half-strength MS medium with 1% (w/v) Suc and 0.7% (w/v) agar supplemented with GA_3 (Gibco Laboratories; catalog no. 890134011) and/or 24-epibrassinolide (Sigma; catalog no. E1641). *VUP1 OX* or wild-type seeds were planted on the same plates to reduce growth condition variation. For *VUP1 OX* plants, truncated and mutated versions of *VUP1* and *VUP1* homologs in pEarley Gate 101 or pEarley Gate 104, T0 seeds were sown directly on soil, grown for 1 week, and selected with a 120 μg mL^{-1} solution of BASTA (Liberty 150; Bayer CropScience). After 1 week, resistant T1 plants were transferred to individual pots. Whole-seedling and whole-plant images were taken with a Nikon D90 digital camera.

Isolation of *vup1* Mutants

T-DNA insertion lines in *VUP1* in Col-0, *vup1-1* (Salk_073777C), and *vup1-2* (Salk_028468) were obtained from the Arabidopsis Biological Resource Center (Alonso et al., 2003). T-DNA insertions were confirmed by PCR and subsequent sequencing. Homozygote populations for each mutant were obtained by PCR-based genotyping using the primers listed in Supplemental Table S2.

Cloning and Plant Transformation

VUP1 complete coding sequences or truncated *VUP1* versions were amplified from mixed tissue cDNAs. Arabidopsis *VUP1* homologous genes were PCR amplified from Arabidopsis genomic DNA. Poplar (*Populus trichocarpa*) *VUP1* homologs were PCR amplified from mixed xylem/leaf cDNAs from poplar. *Brachypodium distachyon* and *Selaginella moellendorffii* homologs were amplified from corresponding genomic DNA samples. Sequences of all the primers used for PCR amplifications can be found in Supplemental Table S2. PCR products were subcloned into pCR8/GW/TOPO using LR Clonase (Life Technologies) into the binary vector pEarley Gate 101. *VUP1* truncated versions were transferred into the binary vector pEarley Gate 104. *VUP1* coding sequence (CDS) was transferred into both pEarley Gate 101 and 104. For site-directed mutagenesis, two overlapping PCR products were amplified using a forward and a reverse primer containing the mutated codon(s) and the corresponding forward and reverse primers of *VUP1* CDS (for primer sequences, see Supplemental Table S2). The two amplicons were gel purified and used as templates for a third PCR (Invitrogen) and confirmed by sequencing. *VUP1* homologs and mutated *VUP1* versions were transferred using forward and reverse primers of *VUP1* CDS. Mutated CDS were subcloned into pCR8/GW/TOPO (Invitrogen), confirmed by sequencing, and transferred by LR recombination into the binary vector pEarley Gate 101. For the *promVUP:VUP1:GUS* construct, a 3.2-kb Arabidopsis genomic DNA fragment, containing 2 kb 5′ to the *VUP1* translation start site and the *VUP1* genic sequence up to the stop codon, was PCR amplified and subcloned into pCR8/GW/TOPO (Invitrogen) and then transferred by recombination into the pGWB3 binary vector. All constructs were introduced into Arabidopsis by *Agrobacterium tumefaciens* (strain GV3101)-mediated in planta transformation (Clough and Bent, 1998). The mCherry-VirD2NLS inserted into pK2GW7 was obtained from Dr. M. Schuetz.

Sequence Collection and Analysis

VUP1 homologous sequences were identified by searching genomic and EST databases using the BLASTP or TBLASTN program (Altschul et al., 1997) and selected based on overall similarity and the presence of conserved residues. Deduced amino acid sequences were aligned in MUSCLE 3.7 (Edgar, 2004a) using default parameters (sequencing clustering, Unweighted Pair Group Method with Arithmetic Mean; objective score, classic sum-of-pairs score). The gene identifiers of the representative sequences used for multialignment for individual *VUP1* homologs are as follows: Arabidopsis *VUP1* (At3g21710), *VUP2* (AT1G50930), *VUP3* (At3g20557), and *VUP4* (At5g54790); *Oryza sativa* (LOC_Os07g34020); poplar Pt1 (POPTR_0002s23090), Pt2 (POPTR_0014s15000), Pt3 (POPTR_0001s44530), and Pt4 (POPTR_0011s13900); *S. moellendorffii* (fgenesh2_pg.C_scaffold_9000114); *B. distachyon* (Bradi1g25990); and *Zea mays* (GRMZM2G009144). National Center for Biotechnology Information identifiers of the representative sequences for individual VUP1 homologs are as follows: *Glycine max* (XP_003540311.1), *Vitis vinifera* (XP_002279953.1), and *Ricinus communis* (RCOM_0485560 and XP_002522866.1). All sequences obtained are given in Supplemental Figure S6.

Microscopy

Hand sections from inflorescence stems of 6- to 8-week-old Arabidopsis plants were stained with 2% (w/v) phloroglucinol for 30 s and mounted on

microscope slides with concentrated HCl. Observations were made with an Olympus AX70 light microscope. For hypocotyl cell length measurements, 5-d-old dark-grown seedlings were mounted on slides in water. Imaging was performed using a Nikon PCM 2000 confocal microscope equipped with a Leica oil-immersion 63× Plan-Apo objective (numerical aperture 1.4) using the differential interference contrast settings. At least 10 seedlings from two independent *VUP1 OX* T2 lines were used for each assay. ImageJ (http://rsbweb.nih.gov/ij/) was used to quantify epidermal cell lengths.

GUS Staining

For histochemical staining of GUS activity, samples were vacuum infiltrated in 50 mM sodium phosphate buffer (pH 7) containing 3 mM ferrocyanide, 3 mM ferricyanide, 10 mM EDTA, 0.01% (v/v) Triton X-100, and 1.5 mM 5-bromo-4-chloro-3-indolyl-β-glucuronic acid substrate for 30 min before incubation overnight at 37°C. After successive washes with 50%, 70%, and 96% (v/v) ethanol solutions, tissues were directly observed with a stereomicroscope (MZ16FA; Leica Microsystems) or a microscope (Olympus AX70).

Fluorescence Microscopy

VUP1 CDS in pEarley Gate 101 (*VUP1 OX*) or pEarley Gate 104 were used for fluorescence microscopy. The mCherry-VirD2NLS inserted into pK2GW7 was used as a nuclear marker. For transient expression, leaves of 4-week-old *Nicotiana benthamiana* plants were agroinfiltrated and subsequently placed in a growth chamber for 96 h. Observation of *VUP1:YFP* in Arabidopsis was done with 2-week-old leaves of *VUP1 OX* T2 plants preincubated in a 0.5% (w/v) propidium iodide in 50 mM phosphate buffer at room temperature for 10 min. Most imaging was performed using a Nikon PCM 2000 confocal microscope equipped with a Leica oil-immersion 63× Plan-Apo objective (numerical aperture 1.4) with the following excitation/emission filters: YFP (514/540), RED FLUORESCENT PROTEIN (561/595), and propidium iodide (620/720). ImageJ (http://rsbweb.nih.gov/ij/) software were used to create maximum projections.

RNA Isolation and RT-PCR Gene Expression Analysis

Plant samples were homogenized in liquid nitrogen, and TRIzol reagent (Invitrogen; 1 mL of TRIzol per 100 mg of tissue) was used for RNA isolation, treated with DNaseI (Invitrogen), RNA purified with the RNeasy Mini Kit (Qiagen) as recommended by the manufacturers, and then stored at −80°C before use. RT was performed as described (Kim et al., 2010). For RT-PCR, gene-specific primers (Supplemental Table S2) were used in PCR to amplify the corresponding cDNA sequences under the following PCR conditions: 95°C for 30 s, followed by 31 cycles of 95°C for 30 s, 56°C for 30 s, and 68°C for 30 s, followed by 68°C for 10 min, using Taq polymerase in a 25-μL total reaction volume. *ACTIN2* (*At3g18780*) was used as a reference gene.

Microarray Expression Profiling

Three biological replicates, consisting of three independent *VUP1 OX* lines (T2 generation) and wild-type lines grown separately, were used for RNA extraction. RNA concentrations and integrity were analyzed with a 2100 Bioanalyzer (Agilent Technologies). RT and labeling, array hybridization, microarray scanning, and microarray data analysis were as described (Hall and Ellis, 2013) except that 30 μg of total RNA was used.

Supplemental Data

The following materials are available in the online version of this article.

Supplemental Figure S1. Amino acid sequence alignment of 62 VUP1 homologs using the ClustalW program.

Supplemental Figure S2. Amino acid sequence alignment of selected VUP1 homologs and selected Arabidopsis bHLH transcription factors using the MUSCLE 3.7 program.

Supplemental Figure S3. Degradation pattern of VUP1:YFP overexpressed in Arabidopsis leaves.

Supplemental Figure S4. Light microscopy analysis of epidermal cells from etiolated hypocotyls of 5-d-old seedlings.

Supplemental Figure S5. Immunoblot analysis of mutated VUP1 overexpressors.

Supplemental Figure S6. Amino acid sequences of VUP1 homologs used for multialignment.

Supplemental Table S1. Genes significantly up-regulated and down-regulated (fold change > 1.5, $P < 0.01$) in *VUP1 OX* versus the wild type.

Supplemental Table S2. List of primers used for cloning, RT-PCR, and genotyping.

ACKNOWLEDGMENTS

We thank the Arabidopsis Biological Resource Center and The Arabidopsis Information Resource for providing the Arabidopsis T-DNA insertion mutants. We thank Dr. Mathias Schuetz (University of British Columbia) for thoughtful discussions and comments on the manuscript and for providing the mCherry-VirD2NLS inserted into pK2GW7 vector and Brian Ellis (University of British Columbia) for advice on phosphomutant strategies. We thank Dr. Clint Chapple (Purdue University) for providing the *S. moellendorffii* genomic DNA and Rachel Yoon (University of British Columbia) for technical assistance.

Received January 22, 2014; accepted February 22, 2014; published February 24, 2014.

LITERATURE CITED

Alonso JM, Stepanova AN, Leisse TJ, Kim CJ, Chen H, Shinn P, Stevenson DK, Zimmerman J, Barajas P, Cheuk R, et al (2003) Genome-wide insertional mutagenesis of *Arabidopsis thaliana*. Science **301:** 653–657

Altschul SF, Madden TL, Schäffer AA, Zhang J, Zhang Z, Miller W, Lipman DJ (1997) Gapped BLAST and PSI-BLAST: a new generation of protein database search programs. Nucleic Acids Res **25:** 3389–3402

Arabidopsis Genome Initiative (2000) Analysis of the genome sequence of the flowering plant *Arabidopsis thaliana*. Nature **408:** 796–815

Arabidopsis Interactome Mapping Consortium (2011) Evidence for network evolution in an Arabidopsis interactome map. Science **333:** 601–607

Bai MY, Fan M, Oh E, Wang ZY (2012a) A triple helix-loop-helix/basic helix-loop-helix cascade controls cell elongation downstream of multiple hormonal and environmental signaling pathways in *Arabidopsis*. Plant Cell **24:** 4917–4929

Bai MY, Shang JX, Oh E, Fan M, Bai Y, Zentella R, Sun TP, Wang ZY (2012b) Brassinosteroid, gibberellin and phytochrome impinge on a common transcription module in Arabidopsis. Nat Cell Biol **14:** 810–817

Bao H, Li E, Mansfield SD, Cronk QC, El-Kassaby YA, Douglas CJ (2013) The developing xylem transcriptome and genome-wide analysis of alternative splicing in *Populus trichocarpa* (black cottonwood) populations. BMC Genomics **14:** 359

Bendtsen JD, Nielsen H, von Heijne G, Brunak S (2004) Improved prediction of signal peptides: SignalP 3.0. J Mol Biol **340:** 783–795

Bishop GJ, Koncz C (2002) Brassinosteroids and plant steroid hormone signaling. Plant Cell (Suppl) **14:** S97–S110

Brown D, Wightman R, Zhang Z, Gomez LD, Atanassov I, Bukowski JP, Tryfona T, McQueen-Mason SJ, Dupree P, Turner S (2011) Arabidopsis genes *IRREGULAR XYLEM* (*IRX15*) and *IRX15L* encode DUF579-containing proteins that are essential for normal xylan deposition in the secondary cell wall. Plant J **66:** 401–413

Brown DM, Goubet F, Wong VW, Goodacre R, Stephens E, Dupree P, Turner SR (2007) Comparison of five xylan synthesis mutants reveals new insight into the mechanisms of xylan synthesis. Plant J **52:** 1154–1168

Brown DM, Zeef LA, Ellis J, Goodacre R, Turner SR (2005) Identification of novel genes in *Arabidopsis* involved in secondary cell wall formation using expression profiling and reverse genetics. Plant Cell **17:** 2281–2295

Brown DM, Zhang Z, Stephens E, Dupree P, Turner SR (2009) Characterization of IRX10 and IRX10-like reveals an essential role in glucuronoxylan biosynthesis in Arabidopsis. Plant J **57:** 732–746

Busse JS, Evert RF (1999a) Pattern of differentiation of the first vascular elements in the embryo and seedling of *Arabidopsis thaliana*. Int J Plant Sci **160:** 1–13

Busse JS, Evert RF (1999b) Vascular differentiation and transition in the seedling of *Arabidopsis thaliana* (Brassicaceae). Int J Plant Sci **160:** 241–251

Caño-Delgado A, Yin Y, Yu C, Vafeados D, Mora-García S, Cheng JC, Nam KH, Li J, Chory J (2004) BRL1 and BRL3 are novel brassinosteroid receptors that function in vascular differentiation in Arabidopsis. Development **131:** 5341–5351

Cao D, Cheng H, Wu W, Soo HM, Peng J (2006) Gibberellin mobilizes distinct DELLA-dependent transcriptomes to regulate seed germination and floral development in Arabidopsis. Plant Physiol **142:** 509–525

Choe SW, Noguchi T, Fujioka S, Takatsuto S, Tissier CP, Gregory BD, Ross AS, Tanaka A, Yoshida S, Tax FE, et al (1999) The *Arabidopsis dwf7/ste1* mutant is defective in the delta7 sterol C-5 desaturation step leading to brassinosteroid biosynthesis. Plant Cell **11:** 207–221

Clough SJ, Bent AF (1998) Floral dip: a simplified method for Agrobacterium-mediated transformation of *Arabidopsis thaliana*. Plant J **16:** 735–743

Clouse SD, Langford M, McMorris TC (1996) A brassinosteroid-insensitive mutant in *Arabidopsis thaliana* exhibits multiple defects in growth and development. Plant Physiol **111:** 671–678

Cohen JD, Meudt WJ (1983) Investigations of the mechanism of the brassinosteroid response. I. Indole-3-acetic-acid metabolism and transport. Plant Physiol **72:** 691–694

Dayan J, Voronin N, Gong F, Sun TP, Hedden P, Fromm H, Aloni R (2012) Leaf-induced gibberellin signaling is essential for internode elongation, cambial activity, and fiber differentiation in tobacco stems. Plant Cell **24:** 66–79

Durek P, Schmidt R, Heazlewood JL, Jones A, MacLean D, Nagel A, Kersten B, Schulze WX (2010) PhosPhAt: the Arabidopsis thaliana phosphorylation site database. An update. Nucleic Acids Res **38:** D828–D834

Edgar RC (2004a) MUSCLE: a multiple sequence alignment method with reduced time and space complexity. BMC Bioinformatics **5:** 113

Edgar RC (2004b) MUSCLE: multiple sequence alignment with high accuracy and high throughput. Nucleic Acids Res **32:** 1792–1797

Eshed Y, Baum SF, Perea JV, Bowman JL (2001) Establishment of polarity in lateral organs of plants. Curr Biol **11:** 1251–1260

Fujioka S, Li J, Choi YH, Seto H, Takatsuto S, Noguchi T, Watanabe T, Kuriyama H, Yokota T, Chory J, et al (1997) The *Arabidopsis deetiolated2* mutant is blocked early in brassinosteroid biosynthesis. Plant Cell **9:** 1951–1962

Fukuda H (2004) Signals that control plant vascular cell differentiation. Nat Rev Mol Cell Biol **5:** 379–391

Gallego-Bartolomé J, Minguet EG, Grau-Enguix F, Abbas M, Locascio A, Thomas SG, Alabadí D, Blázquez MA (2012) Molecular mechanism for the interaction between gibberellin and brassinosteroid signaling pathways in Arabidopsis. Proc Natl Acad Sci USA **109:** 13446–13451

Gazzarrini S, McCourt P (2003) Cross-talk in plant hormone signalling: what Arabidopsis mutants are telling us. Ann Bot (Lond) **91:** 605–612

Goda H, Sasaki E, Akiyama K, Maruyama-Nakashita A, Nakabayashi K, Li W, Ogawa M, Yamauchi Y, Preston J, Aoki K, et al (2008) The AtGenExpress hormone and chemical treatment data set: experimental design, data evaluation, model data analysis and data access. Plant J **55:** 526–542

Goda H, Sawa S, Asami T, Fujioka S, Shimada Y, Yoshida S (2004) Comprehensive comparison of auxin-regulated and brassinosteroid-regulated genes in Arabidopsis. Plant Physiol **134:** 1555–1573

Goodstein DM, Shu S, Howson R, Neupane R, Hayes RD, Fazo J, Mitros T, Dirks W, Hellsten U, Putnam N, et al (2012) Phytozome: a comparative platform for green plant genomics. Nucleic Acids Res **40:** D1178–D1186

Grienenberger E, Kim SS, Lallemand B, Geoffroy P, Heintz D, Souza CdA, Heitz T, Douglas CJ, Legrand M (2010) Analysis of *TETRAKETIDE α-PYRONE REDUCTASE* function in *Arabidopsis thaliana* reveals a previously unknown, but conserved, biochemical pathway in sporopollenin monomer biosynthesis. Plant Cell **22:** 4067–4083

Hall H, Ellis B (2013) Transcriptional programming during cell wall maturation in the expanding Arabidopsis stem. BMC Plant Biol **13:** 14

Hoffmann L, Besseau S, Geoffroy P, Ritzenthaler C, Meyer D, Lapierre C, Pollet B, Legrand M (2004) Silencing of hydroxycinnamoyl-coenzyme A shikimate/quinate hydroxycinnamoyltransferase affects phenylpropanoid biosynthesis. Plant Cell **16:** 1446–1465

Hörnblad E, Ulfstedt M, Ronne H, Marchant A (2013) Partial functional conservation of IRX10 homologs in Physcomitrella patens and Arabidopsis thaliana indicates an evolutionary step contributing to vascular formation in land plants. BMC Plant Biol **13:** 3

Hu W, Ma H (2006) Characterization of a novel putative zinc finger gene MIF1: involvement in multiple hormonal regulation of Arabidopsis development. Plant J **45:** 399–422

Hyun Y, Lee I (2006) KIDARI, encoding a non-DNA binding bHLH protein, represses light signal transduction in Arabidopsis thaliana. Plant Mol Biol **61:** 283–296

Ikeda M, Fujiwara S, Mitsuda N, Ohme-Takagi M (2012) A triantagonistic basic helix-loop-helix system regulates cell elongation in *Arabidopsis*. Plant Cell **24:** 4483–4497

Ilegems M, Douet V, Meylan-Bettex M, Uyttewaal M, Brand L, Bowman JL, Stieger PA (2010) Interplay of auxin, KANADI and class III HD-ZIP transcription factors in vascular tissue formation. Development **137:** 975–984

Jaillais Y, Vert G (2012) Brassinosteroids, gibberellins and light-mediated signalling are the three-way controls of plant sprouting. Nat Cell Biol **14:** 788–790

Jensen JK, Kim H, Cocuron JC, Orler R, Ralph J, Wilkerson CG (2011) The DUF579 domain containing proteins IRX15 and IRX15-L affect xylan synthesis in Arabidopsis. Plant J **66:** 387–400

Jones L, Ennos AR, Turner SR (2001) Cloning and characterization of irregular xylem4 (irx4): a severely lignin-deficient mutant of Arabidopsis. Plant J **26:** 205–216

Katsumi M (1985) Interaction of a brassinosteroid with IAA and GA3 in the elongation of cucumber hypocotyl sections. Plant Cell Physiol **26:** 615–625

Kauschmann A, Jessop A, Koncz C, Szekeres M, Willmitzer L, Altmann T (1996) Genetic evidence for an essential role of brassinosteroids in plant development. Plant J **9:** 701–713

Kim SS, Grienenberger E, Lallemand B, Colpitts CC, Kim SY, Souza CdA, Geoffroy P, Heintz D, Krahn D, Kaiser M, et al (2010) *LAP6/POLYKETIDE SYNTHASE A* and *LAP5/POLYKETIDE SYNTHASE B* encode hydroxyalkyl α-pyrone synthases required for pollen development and sporopollenin biosynthesis in *Arabidopsis thaliana*. Plant Cell **22:** 4045–4066

Kim TW, Wang ZY (2010) Brassinosteroid signal transduction from receptor kinases to transcription factors. Annu Rev Plant Biol **61:** 681–704

Krogh A, Larsson B, von Heijne G, Sonnhammer EL (2001) Predicting transmembrane protein topology with a hidden Markov model: application to complete genomes. J Mol Biol **305:** 567–580

Kubo M, Udagawa M, Nishikubo N, Horiguchi G, Yamaguchi M, Ito J, Mimura T, Fukuda H, Demura T (2005) Transcription switches for protoxylem and metaxylem vessel formation. Genes Dev **19:** 1855–1860

Lamesch P, Berardini TZ, Li DH, Swarbreck D, Wilks C, Sasidharan R, Muller R, Dreher K, Alexander DL, Garcia-Hernandez M, et al (2012) The Arabidopsis Information Resource (TAIR): improved gene annotation and new tools. Nucleic Acids Res **40:** D1202–D1210

Lee C, Zhong R, Richardson EA, Himmelsbach DS, McPhail BT, Ye ZH (2007) The PARVUS gene is expressed in cells undergoing secondary wall thickening and is essential for glucuronoxylan biosynthesis. Plant Cell Physiol **48:** 1659–1672

Lee S, Lee S, Yang KY, Kim YM, Park SY, Kim SY, Soh MS (2006a) Overexpression of PRE1 and its homologous genes activates gibberellin-dependent responses in Arabidopsis thaliana. Plant Cell Physiol **47:** 591–600

Lee YK, Kim GT, Kim IJ, Park J, Kwak SS, Choi G, Chung WI (2006b) LONGIFOLIA1 and LONGIFOLIA2, two homologous genes, regulate longitudinal cell elongation in Arabidopsis. Development **133:** 4305–4314

Li E, Bhargava A, Qiang W, Friedmann MC, Forneris N, Savidge RA, Johnson LA, Mansfield SD, Ellis BE, Douglas CJ (2012) The class II KNOX gene KNAT7 negatively regulates secondary wall formation in Arabidopsis and is functionally conserved in Populus. New Phytol **194:** 102–115

Lin PC, Pomeranz MC, Jikumaru Y, Kang SG, Hah C, Fujioka S, Kamiya Y, Jang JC (2011) The Arabidopsis tandem zinc finger protein AtTZF1 affects ABA- and GA-mediated growth, stress and gene expression responses. Plant J **65:** 253–268

Milhinhos A, Miguel CM (2013) Hormone interactions in xylem development: a matter of signals. Plant Cell Rep **32:** 867–883

Nagata N, Asami T, Yoshida S (2001) Brassinazole, an inhibitor of brassinosteroid biosynthesis, inhibits development of secondary xylem in cress plants (*Lepidium sativum*). Plant Cell Physiol **42:** 1006–1011

Nemhauser JL, Mockler TC, Chory J (2004) Interdependency of brassinosteroid and auxin signaling in Arabidopsis. PLoS Biol **2:** E258

Oh E, Zhu JY, Wang ZY (2012) Interaction between BZR1 and PIF4 integrates brassinosteroid and environmental responses. Nat Cell Biol **14:** 802–809

Ohashi-Ito K, Demura T, Fukuda H (2002) Promotion of transcript accumulation of novel Zinnia immature xylem-specific HD-Zip III homeobox genes by brassinosteroids. Plant Cell Physiol **43:** 1146–1153

Ohashi-Ito K, Fukuda H (2003) HD-zip III homeobox genes that include a novel member, ZeHB-13 (Zinnia)/ATHB-15 (Arabidopsis), are involved in procambium and xylem cell differentiation. Plant Cell Physiol **44:** 1350–1358

Ohashi-Ito K, Kubo M, Demura T, Fukuda H (2005) Class III homeodomain leucine-zipper proteins regulate xylem cell differentiation. Plant Cell Physiol **46:** 1646–1656

Ohashi-Ito K, Oda Y, Fukuda H (2010) *Arabidopsis* VASCULAR-RELATED NAC-DOMAIN6 directly regulates the genes that govern programmed cell death and secondary wall formation during xylem differentiation. Plant Cell **22:** 3461–3473

Oikawa A, Joshi HJ, Rennie EA, Ebert B, Manisseri C, Heazlewood JL, Scheller HV (2010) An integrative approach to the identification of Arabidopsis and rice genes involved in xylan and secondary wall development. PLoS ONE **5:** e15481

Peña MJ, Zhong R, Zhou GK, Richardson EA, O'Neill MA, Darvill AG, York WS, Ye ZH (2007) *Arabidopsis irregular xylem8* and *irregular xylem9*: implications for the complexity of glucuronoxylan biosynthesis. Plant Cell **19:** 549–563

Persson S, Caffall KH, Freshour G, Hilley MT, Bauer S, Poindexter P, Hahn MG, Mohnen D, Somerville C (2007) The *Arabidopsis irregular xylem8* mutant is deficient in glucuronoxylan and homogalacturonan, which are essential for secondary cell wall integrity. Plant Cell **19:** 237–255

Persson S, Wei HR, Milne J, Page GP, Somerville CR (2005) Identification of genes required for cellulose synthesis by regression analysis of public microarray data sets. Proc Natl Acad Sci USA **102:** 8633–8638

Ragni L, Nieminen K, Pacheco-Villalobos D, Sibout R, Schwechheimer C, Hardtke CS (2011) Mobile gibberellin directly stimulates *Arabidopsis* hypocotyl xylem expansion. Plant Cell **23:** 1322–1336

Reed JW, Nagatani A, Elich TD, Fagan M, Chory J (1994) Phytochrome A and phytochrome B have overlapping but distinct functions in Arabidopsis development. Plant Physiol **104:** 1139–1149

Ruzinova MB, Benezra R (2003) Id proteins in development, cell cycle and cancer. Trends Cell Biol **13:** 410–418

Rymen B, Sugimoto K (2012) Tuning growth to the environmental demands. Curr Opin Plant Biol **15:** 683–690

Sachs T (1981) The control of vascular development. Adv Bot Res **9:** 151–262

Sachs T (1991) Cell polarity and tissue patterning in plants. Development **113:** 83–93

Sala C, Sala F (1985) Effect of brassinosteroid on cell division and enlargement in cultured carrot (Daucus carota L.) cells. Plant Cell Rep **4:** 144–147

Schuetz M, Smith R, Ellis B (2013) Xylem tissue specification, patterning, and differentiation mechanisms. J Exp Bot **64:** 11–31

Steeves TA, Sussex IM (1989) Patterns in Plant Development. Cambridge University Press, Cambridge, UK

Sun T, Goodman HM, Ausubel FM (1992) Cloning the *Arabidopsis GA1* locus by genomic subtraction. Plant Cell **4:** 119–128

Sun TP (2011) The molecular mechanism and evolution of the GA-GID1-DELLA signaling module in plants. Curr Biol **21:** R338–R345

Sun Y, Fan XY, Cao DM, Tang W, He K, Zhu JY, He JX, Bai MY, Zhu S, Oh E, et al (2010) Integration of brassinosteroid signal transduction with the transcription network for plant growth regulation in Arabidopsis. Dev Cell **19:** 765–777

Szekeres M, Németh K, Koncz-Kálmán Z, Mathur J, Kauschmann A, Altmann T, Rédei GP, Nagy F, Schell J, Koncz C (1996) Brassinosteroids rescue the deficiency of CYP90, a cytochrome P450, controlling cell elongation and de-etiolation in Arabidopsis. Cell **85:** 171–182

Taylor NG, Scheible WR, Cutler S, Somerville CR, Turner SR (1999) The *irregular xylem3* locus of Arabidopsis encodes a cellulose synthase required for secondary cell wall synthesis. Plant Cell **11:** 769–780

Tokunaga N, Uchimura N, Sato Y (2006) Involvement of gibberellin in tracheary element differentiation and lignification in Zinnia elegans xylogenic culture. Protoplasma **228:** 179–187

Toufighi K, Brady SM, Austin R, Ly E, Provart NJ (2005) The Botany Array Resource: e-northerns, expression angling, and promoter analyses. Plant J **43:** 153–163

Turner SR, Somerville CR (1997) Collapsed xylem phenotype of *Arabidopsis* identifies mutants deficient in cellulose deposition in the secondary cell wall. Plant Cell **9:** 689–701

Ubeda-Tomas S, Edvardsson E, Eland C, Singh SK, Zadik D, Aspeborg H, Gorzsas A, Teeri TT, Sundberg B, Persson P, et al (2007) Genomic-assisted identification of genes involved in secondary growth in Arabidopsis utilising transcript profiling of poplar wood-forming tissues. Physiol Plant **129:** 415–428

Wang H, Zhu Y, Fujioka S, Asami T, Li J, Li J (2009) Regulation of *Arabidopsis* brassinosteroid signaling by atypical basic helix-loop-helix proteins. Plant Cell **21:** 3781–3791

Wang X, Bian Y, Cheng K, Gu LF, Ye M, Zou H, Sun SS, He JX (2013) A large-scale protein phosphorylation analysis reveals novel phosphorylation motifs and phosphoregulatory networks in Arabidopsis. J Proteomics **78:** 486–498

Wang ZY, Nakano T, Gendron J, He J, Chen M, Vafeados D, Yang Y, Fujioka S, Yoshida S, Asami T, et al (2002) Nuclear-localized BZR1 mediates brassinosteroid-induced growth and feedback suppression of brassinosteroid biosynthesis. Dev Cell **2:** 505–513

Weng JK, Chapple C (2010) The origin and evolution of lignin biosynthesis. New Phytol **187:** 273–285

Wu AM, Rihouey C, Seveno M, Hörnblad E, Singh SK, Matsunaga T, Ishii T, Lerouge P, Marchant A (2009) The Arabidopsis IRX10 and IRX10-LIKE glycosyltransferases are critical for glucuronoxylan biosynthesis during secondary cell wall formation. Plant J **57:** 718–731

Yamaguchi M, Goué N, Igarashi H, Ohtani M, Nakano Y, Mortimer JC, Nishikubo N, Kubo M, Katayama Y, Kakegawa K, et al (2010) VASCULAR-RELATED NAC-DOMAIN6 and VASCULAR-RELATED NAC-DOMAIN7 effectively induce transdifferentiation into xylem vessel elements under control of an induction system. Plant Physiol **153:** 906–914

Yamaguchi M, Kubo M, Fukuda H, Demura T (2008) VASCULAR-RELATED NAC-DOMAIN7 is involved in the differentiation of all types of xylem vessels in Arabidopsis roots and shoots. Plant J **55:** 652–664

Yamaguchi M, Mitsuda N, Ohtani M, Ohme-Takagi M, Kato K, Demura T (2011) VASCULAR-RELATED NAC-DOMAIN7 directly regulates the expression of a broad range of genes for xylem vessel formation. Plant J **66:** 579–590

Yamamoto R, Demura T, Fukuda H (1997) Brassinosteroids induce entry into the final stage of tracheary element differentiation in cultured Zinnia cells. Plant Cell Physiol **38:** 980–983

Yamamoto R, Fujioka S, Demura T, Takatsuto S, Yoshida S, Fukuda H (2001) Brassinosteroid levels increase drastically prior to morphogenesis of tracheary elements. Plant Physiol **125:** 556–563

Yamamoto R, Fujioka S, Iwamoto K, Demura T, Takatsuto S, Yoshida S, Fukuda H (2007) Co-regulation of brassinosteroid biosynthesis-related genes during xylem cell differentiation. Plant Cell Physiol **48:** 74–83

Yin Y, Wang ZY, Mora-Garcia S, Li J, Yoshida S, Asami T, Chory J (2002) BES1 accumulates in the nucleus in response to brassinosteroids to regulate gene expression and promote stem elongation. Cell **109:** 181–191

Zhang LY, Bai MY, Wu J, Zhu JY, Wang H, Zhang Z, Wang W, Sun Y, Zhao J, Sun X, et al (2009) Antagonistic HLH/bHLH transcription factors mediate brassinosteroid regulation of cell elongation and plant development in rice and *Arabidopsis*. Plant Cell **21:** 3767–3780

Zhong R, Peña MJ, Zhou GK, Nairn CJ, Wood-Jones A, Richardson EA, Morrison WH III, Darvill AG, York WS, Ye ZH (2005) *Arabidopsis fragile fiber8*, which encodes a putative glucuronyltransferase, is essential for normal secondary wall synthesis. Plant Cell **17:** 3390–3408

Zhong RQ, Lee CH, Ye ZH (2010a) Evolutionary conservation of the transcriptional network regulating secondary cell wall biosynthesis. Trends Plant Sci **15:** 625–632

Zhong RQ, Lee CH, Ye ZH (2010b) Global analysis of direct targets of secondary wall NAC master switches in Arabidopsis. Mol Plant **3:** 1087–1103

Zhong RQ, Lee CH, Zhou JL, McCarthy RL, Ye ZH (2008) A battery of transcription factors involved in the regulation of secondary cell wall biosynthesis in *Arabidopsis*. Plant Cell **20:** 2763–2782